PART I
Vascular Imaging Techniques and Physiologic Testing

CHAPTER 1
Arterial and Venous Duplex Scanning

Gregory L. Moneta
Oregon Health and Science University, Portland, OR, USA

The noninvasive vascular laboratory provides the scientific basis for vascular surgery. It safely provides accurate and quantitative evidence of the presence and physiologic significance of arterial and venous disease. In the modern vascular laboratory ultrasound-based techniques, particularly duplex ultrasound techniques, are most extensively employed.

Ultrasound basics

Duplex ultrasound was introduced in 1974 with application to the carotid artery. "Duplex" indicates the technique combines B-mode imaging and Doppler analysis of blood-flow direction and velocity. It is extensively utilized for evaluation of carotid arteries, intra-abdominal arteries and veins, and upper- and lower-extremity arteries and veins. Since its inception, engineering and software advances have been extensive and include: 1) improved gray-scale B-mode imaging, 2) low-frequency scan heads permitting deep penetration of the ultrasound beam from the skin surface, 3) improvements in online computer-based microprocessing, and 4) addition of color-flow imaging.

Color flow is a superimposed real-time colorized image of blood flow onto a standard gray-scale B-mode picture. Echoes from stationary tissues generate B-mode images, whereas those interacting with moving substances (blood) generate a phase shift that is processed separately and color coded to give information on the direction and velocity of blood flow that reflects the magnitude and direction of the Doppler shift. Color flow dramatically reduces the time required to perform duplex examinations by allowing more rapid identification of vessels to be examined. It appears essential for duplex examination of some vessels, such as tibial arteries and veins. Color flow and the ability of modern duplex scanners to detect blood flow velocities <5 cm/s make duplex scanning practical in virtually all areas of the body.

Basics of duplex ultrasound

A vibrating source produces an ultrasonic wave. In duplex ultrasound the vibrating source is the transducer. Ultrasound transducers are contained within scan heads. Scan heads steer and focus the sound beam produced by the transducer. The ultrasound image is derived from the returning echoes and is dependent on precise steering and focusing of the sound beam.

Transducers convert electrical into vibrational energy to produce the ultrasound wave. Transducers can also convert vibrational energy of returning echoes into electrical signals for analysis by the duplex machine's software. The frequency of the vibration is determined by the design of the transducer and determines the wavelength of the sound wave. Frequency and wavelength are related, $\lambda = c/f$, where λ is the wavelength, c is the speed of sound in tissue, and f is the frequency.

Speed of sound in soft tissues averages 1540 m/s. There is little variation in the soft tissues insonated in clinical use of duplex ultrasound. Wavelength is the principle determinant of how well an ultrasound beam penetrates tissue, and wavelength depends on the frequency of the transducer. The transducer frequency is determined by the design of the transducer and is thus controlled by the manufacturer. For examination of the carotid artery, transducer frequencies of 5 to 7.5 MHz provide optimal tissue penetration for clinical purposes.

As noted above, duplex refers to the combination of Doppler and B-mode ("B" stands for "brightness") ultrasound in the same device. Both require analysis of reflected echoes of the original sound beam created by the ultrasound transducer. B-mode analyzes the strength

Haimovici's Vascular Surgery, Sixth Edition. Edited by Enrico Ascher, Frank J. Veith, Peter Gloviczki.

(intensity) and origin of the reflected echo. Doppler analyzes shifts in frequency of the original sound wave produced by the transducer.

B-mode ultrasound

As a sound wave passes through tissue and moves away from the transducer its strength depends upon how much the beam is scattered, attenuated, and reflected. Strength of reflected echoes depend, in part, upon differences in acoustic impedance between media. When there are major differences in acoustic impedance a large proportion of the sound beam is reflected back to the transducer. Small differences in acoustic impedances result in little reflection and the beam continues to propagate through the tissue.

In B-mode ultrasound, the brightness of the individual pixels comprising the ultrasound image is proportional to the strength of the returning echo. This is the ultrasound gray scale, and the resulting image is termed a gray-scale image. Very bright pixels in the gray-scale image indicate large differences in acoustic impedance between media. Less dramatic differences are represented by proportionally less-bright pixels. Thus gallstones, with dramatic differences in acoustic properties from soft tissue, produce strong echoes and proportionally very bright pixels on the ultrasound image, whereas blood, which differs little from soft tissue in acoustic characteristics, often cannot be distinguished from soft tissue with B-mode imaging.

The strength of the reflected echo is also dependent upon the strength of the sound beam at the point where it is relected. Gray-scale images represent the absolute strength of the reflected echo arriving back at the transducer, not the percentage of the beam reflected. Therefore, if the sound beam is very weak at the point of reflection even areas of dramatic acoustic differences will not result in a bright pixel in the B-mode image.

The strength of the ultrasound beam at a specific point also depends on how much the beam has been attenuated passing through tissue. Attenuation depends upon both the tissue traversed and the frequency of the wave. Wave frequency depends upon the frequency of the transducer generating the wave (see discussion above and Equation 1). Higher-frequency sound waves are attenuated more rapidly than lower-frequency sound waves. Higher-frequency transducers therefore provide relatively weak echoes to be reflected from a deep structure. The image generated is comparatively poor compared with a lower-frequency transducer insonating a deeper structure.

Image quality also depends upon linear resolution. Linear resolution is dependent upon the ability to focus the beam. High-frequency sound waves are better focused than sound waves from low-frequency transducers and provide sharper and better quality B-mode images. Image quality is therefore a balance of the strength of the reflected echo and the ability to focus the sound beam. The carotid artery is superficial and higher-frequency transducers can be used to provide clear B-mode images. (Fig. 1.1A and B) Image quality is less when examining deep vessels such as renal or iliac arteries.

Doppler ultrasound

Continuous wave Dopplers have transducers that continually emit vibrations into tissue. Therefore, echoes are also continually reflected back to the transducer. Transducers cannot generate and receive echoes simultaneously. A continuous wave Doppler therefore must have separate transmitters and receivers to generate and receive echoes.

Duplex devices utilize pulse Doppler. Pulse Dopplers use a single transducer to generate and receive echoes. With a pulse Doppler it is possible to know when an

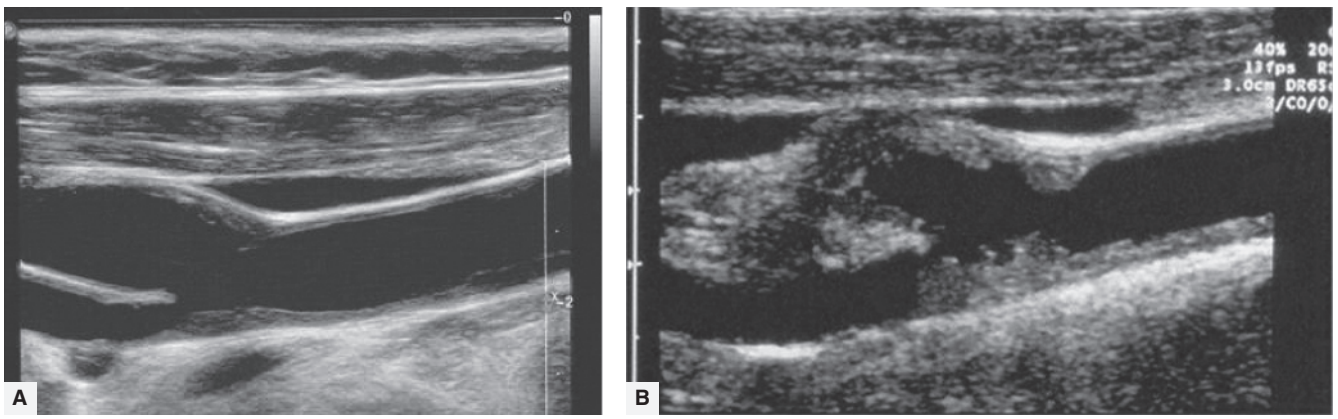

Figure 1.1 Gray-scale images of **(A)** mildly and **(B)** severely diseased bifurcations of the cervical carotid artery.

echo is generated and when it is received. Because the speed of sound is relatively constant in tissue it is therefore possible to tell from what depth a reflected echo originated. The sample volume of the duplex machine is the site from which the returning echo originated. It is determined by specifying the depth from which the pulse Doppler receives reflected echoes.

The transducer of a pulse Doppler is gated, based on the total time from sound-wave generation to arrival of reflected echoes back at the transducer, to receive echoes only from a specified depth, the sample volume. The "position" of the sample volume is determined from the B-mode image. In vascular applications of duplex ultrasound this corresponds to points within the lumen of the vessel examined. B-mode images and Doppler waveforms cannot be generated simultaneously. The B-mode image therefore must be frequently updated during the course of a duplex-ultrasound examination to insure proper placement of the sample volume in the vessel.

When a sound wave encounters moving reflectors, the frequency of the reflected wave changes from that of the original wave generated by the transducer. In vascular ultrasound the moving reflectors are red blood cells. The frequency shift depends upon the velocity of the reflector and its angle with the incident sound beam. The frequency of the original sound wave is known. The frequency of the received echo can be determined by the software of the duplex machine. The velocity of the red blood cells can therefore be calculated provided the angle of the sound beam with the moving reflectors is also known. This relationship is the Doppler equation, $f_r - f_o = [(2f_o v)/c] \cos\theta$, where f_r is the received frequency, f_o is the originating frequency, v is the velocity of the reflector, c is the speed of sound in tissue, and θ is the angle of the incident sound beam with the moving reflectors. θ is termed the "Doppler angle."

Obviously, solving the Doppler equation for the velocity of the moving reflectors requires knowing the Doppler angle. To standardize the results of duplex scanning it is recommended examinations be conducted with a Doppler angle of 60°. At this angle errors in velocity calculations secondary to misreading of the Doppler angle are small as a percentage of the true velocity. When the Doppler angle approaches 70° errors become of greater magnitude because the cosine of θ increases more than linearly. Small errors in determining the Doppler angle when the angle of insonation is <60° have little overall impact on the calculation of the velocity of the moving red cells, making Doppler angles from 45° to 60° acceptable for most clinical studies.

As noted above, pulse Doppler transmits and receives echoes with the same transducer but not at the same time. This dual function results in limits on the frequencies that can be displayed in a spectral waveform. The maximum frequency that can be displayed is half the pulse-transmitting frequency or pulse-repetition frequency (PRF). This is known as the Nyquist limit. If frequencies exceed the Nyquist limit, they are flipped and appear on the reverse-flow side of the spectrum. This is known as "aliasing." If aliasing is encountered, the PRF can be increased to increase the Nyquist limit. The PRF is adjusted by changing the scale of the display or by adjusting the baseline of the display. If aliasing still occurs a lower-frequency transducer or a continuous wave Doppler can be used. Because there are separate transmitting and receiving transducers in a continuous wave Doppler, they are not affected by aliasing.

Color flow

Assigning color to Doppler shifts produces a color-flow image. Returning echoes that are not Doppler shifted are shown in gray scale resulting in color superimposed on a gray-scale image. Color hue and intensity are determined by the direction and magnitude of the Doppler shift. Varying shades of red and blue are used to distinguish flow away from or toward the transducer. By convention, red is generally assigned to arterial flow and blue to venous flow.

At 90° there is no Doppler shift. At 90° the assigned color is black and corresponds to the horizontal black bar serving as the baseline on the color scale that appears on the right side of a color-flow image (Fig. 1.2). Aliasing is manifested on a color-flow image as a mosaic pattern, or as a red-to-blue or blue-to-red transition without an intervening black line. With true reverse flow, blue and red are separated by a black border. Color aliasing can be reduced by increasing the PRF. Power Doppler is a variant of color Doppler, where no direction of flow is assigned to the color image. Velocity information is also not calculated. Detected Doppler shifts are, in effect, colorized without consideration of direction or magnitude of the Doppler shift. Power Doppler is therefore not subject to aliasing or affected by Doppler angle. Power Doppler can detect blood moving at very low velocities and can detect low-flow velocities distal to a very high-grade arterial stenosis. It can outline the course of tortuous vessels and detect flow in small distal veins.

It is tempting to try a direct estimate of the severity of a stenosis from the color-flow image. Such estimates are probably less accurate than measurements of stenosis derived from spectral analysis. Color should serve primarily as a guide for locating vessels and selecting specific sites for examination with the pulse Doppler. Absence of color can indicate severe arterial-wall calcification. In such cases there is also difficulty in obtaining a pulse Doppler waveform.

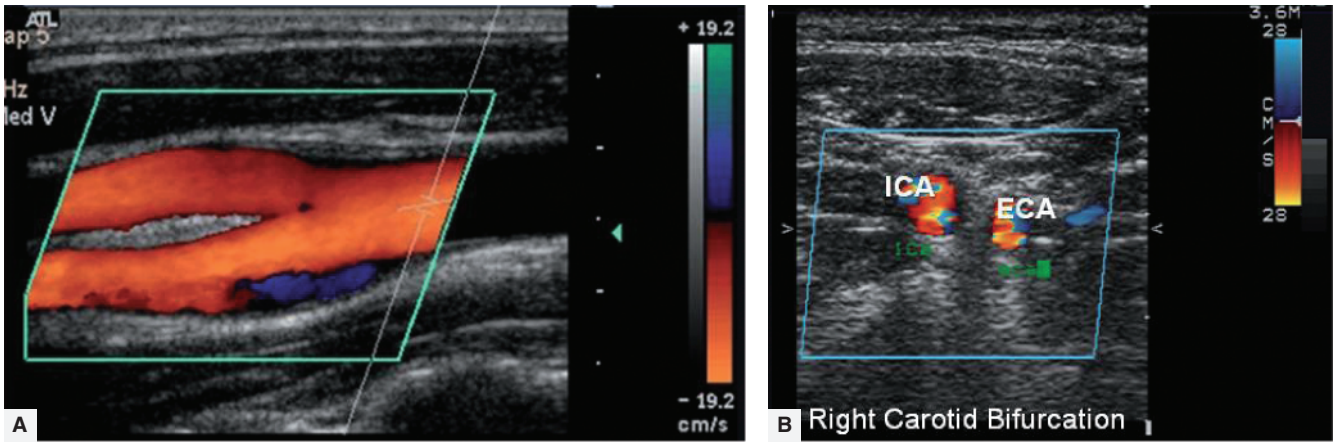

Figure 1.2 **(A)** Color-flow image of a normal carotid bifurcation. The color bar on the right of the image indicates flow towards the probe is blue and away from the probe is red. Note the black line separating the blue and red on the color bar indicates no Doppler shift. Therefore when the color on the image goes from red to black to blue this indicates true flow reversal. The area of reverse flow on the lateral wall of the carotid bulb opposite the flow divider in this image is a normal finding and indicates a carotid bulb free of significant atherosclerosis. **(B)** At the level of the carotid bifurcation the internal carotid artery has a larger diameter than the external carotid artery.

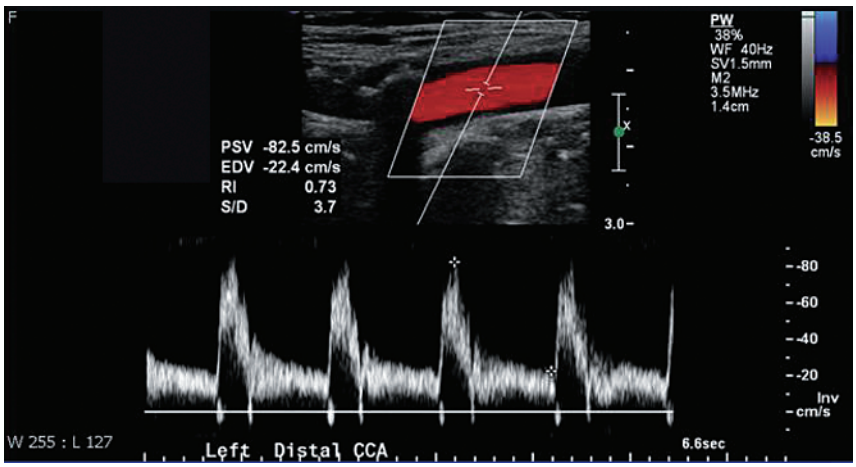

Figure 1.3 A left CCA Doppler waveform. Normally, 80% of CCA flow is directed to the ICA. Normal CCA end-diastolic flow is therefore generally well above baseline and more closely resembles an ICA rather than ECA waveform.

Carotid and vertebral-artery duplex scanning

Duplex diagnosis of internal carotid artery (ICA) stenosis, and arterial stenoses in general, focuses on three areas, the pre-, intra- and post-stenotic regions. Detecting carotid and arterial stenoses involves combinations of spectral analysis, and color and gray-scale imaging. Power Doppler is also selectively used. With arterial duplex, detection of increased-flow velocities within an area of suspected stenosis is of primary importance. Spectral analysis therefore dominates in detection of carotid or any arterial stenosis. However, for distinguishing ICA occlusion from a very high-grade stenosis, power Doppler can identify very low flow in the area of the stenosis, or distal to the stenosis that may not be detected by conventional pulse Doppler. In all cases, the pulsed Doppler and color-flow findings are cross-checked for concordance. Disagreements between the impressions obtained with the color and pulsed Doppler examinations should be reviewed to resolve the discrepancy.

Common carotid-artery waveforms

In the majority of cases, carotid stenosis or occlusion occurs in the proximal ICA. A normal ICA waveform reflects low resistance to blood flow in the cerebral circulation. Low distal resistance is indicated by high flow at the end of the diastolic component of the waveform. Conversely, the external carotid artery (ECA) supplies the higher-resistance circulation of the scalp and face and has a low-end diastolic flow component. Normally 80% of the common carotid-artery (CCA) flow is directed to the ICA. End-diastolic CCA flow is therefore generally well above baseline and exceeds ECA diasto-

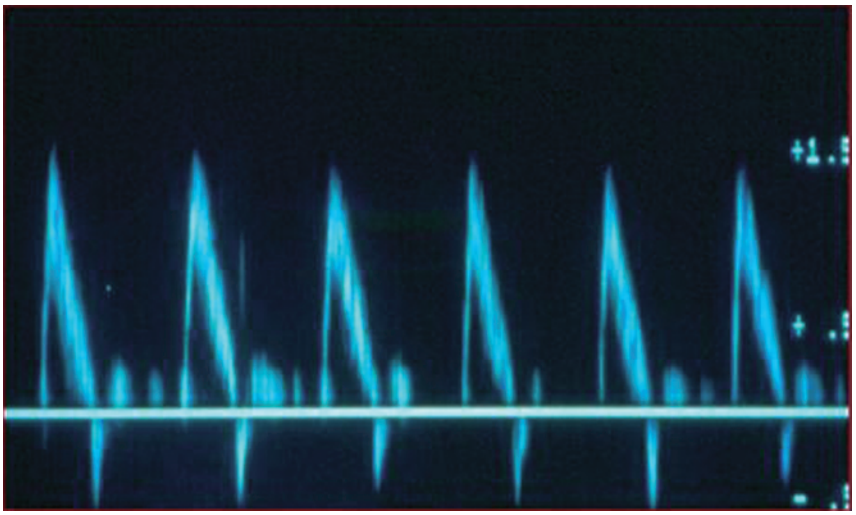

Figure 1.4 Common carotid-artery waveform from a patient with an internal carotid-artery occlusion. There is essentially no end-diastolic flow indicating flow in this common carotid artery is now supplying the high-resistance circulation of the external carotid artery.

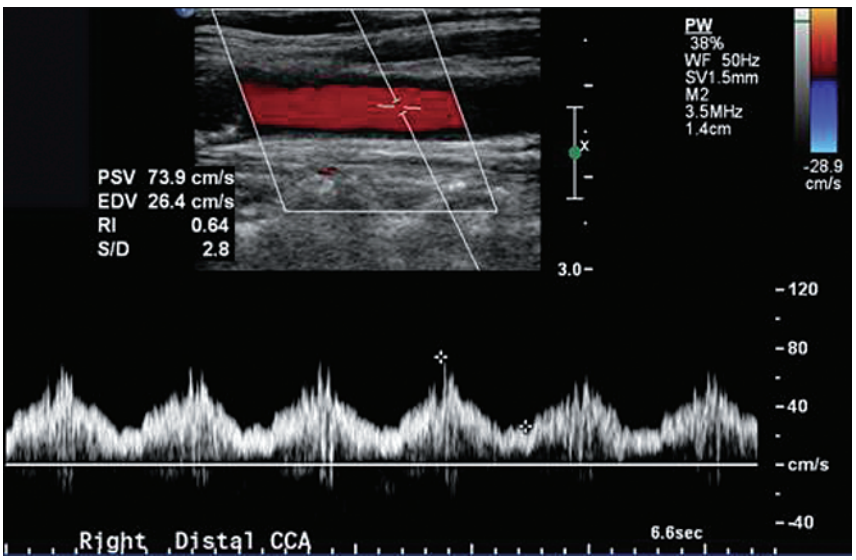

Figure 1.5 Right CCA waveform distal to a high-grade innominate artery stenosis. The systolic upstroke is delayed and the amplitude of the waveform depressed, reflecting the presence of the proximal lesion. Diastolic flow is still well above baseline as the ipsilateral internal carotid artery was not significantly narrowed in this patient.

lic flow. (Fig. 1.3) With very high-grade ICA stenosis or ICA occlusion, outflow is mostly through the higher-resistance external carotid circulation. The CCA waveform then takes on flow resistance of an ECA, with flow to or near zero in end diastole (1) (Fig. 1.4) CCA peak-systolic velocity (PSV) and the overall flow velocity may also be substantially lower than normal. Often solely by observing these changes in the CCA, one can predict high-grade stenosis or occlusion of the ICA.

The CCA contralateral to an ICA occlusion may demonstrate an increased-flow velocity. There is particular elevation of the velocity at the end of diastole, the so-called end-diastolic velocity (EDV), indicating compensatory increase in blood-flow volume in the non-obstructed ICA. This change can be substantial and stenosis-related flow velocities may be artificially elevated on the contralateral side with compensatory high-volume flow (2).

When there is high-grade stenosis at the origin of a CCA or the inominate artery, the ipsilateral CCA waveform may be dampened, with low overall PSV and EDV with a slow rise to peak systole compared with the contralateral CCA waveform (Fig. 1.5). Overall reductions in CCA flow velocity may lower velocities in an ipsilateral ICA stenosis and result in underestimating the severity of ipsilateral ICA stenosis.

Internal carotid-artery waveforms

The normal ICA spectral waveform is indicative of high flow in a low resistant circulation. The systolic upstroke is rapid, PSV is <125 cm/s, and flow is maintained throughout diastole (3). In a normal artery the ICA spectral waveform is clear indicating lack of turbulence. Color shifts, indicating high-velocity flow, and color mosaics, indicating post-stenotic turbulence, aid in selecting examination sites for the pulsed Doppler.

Quantification of ICA-stenosis severity is achieved by analysis of pulsed Doppler spectral waveforms. Measurements are made of peak-systolic and EDV. Comparisons are also made of peak-systolic velocities in the ICA to those in the CCA; the ICA/CCA ratio. PSV is the principal measure of stenosis severity. EDV lags behind, relatively speaking, as stenosis severity progresses. EDV, however, rises rapidly as the stenosis becomes severe (≥60%) (4) (Fig. 1.6). The ICA/CCA ratio is also an excellent measure of stenosis (5). It can serve to compensate for abnormally high-flow and low-flow states that may skew the PSV and EDV up or down.

The sample volume must be placed within the area of greatest stenosis to measure stenosis severity. Color-flow imaging has demonstrated that the orientation of the stenotic jet within a stenosis may not be along the longitudinal axis of the vessel. In areas of mild-to-moderate stenosis, use of a Doppler angle of 60° to the long axis of the vessel is recommended. However, with more severe stenosis the Doppler angle of 60° should be defined by the color-flow-determined long axis of the stenotic flow jet.

Keeping the sample volume small, usually 1.5 mm, allows the operator to detect discrete changes in flow velocity. High velocities may be localized to a small area in the flow stream emanating from the stenosis. A large sample volume that incorporates flow from many points within the vessel in the generation of the spectral waveform may give the false impression of disturbed flow, potentially leading to the misdiagnosis of moderate disease in an otherwise normal vessel.

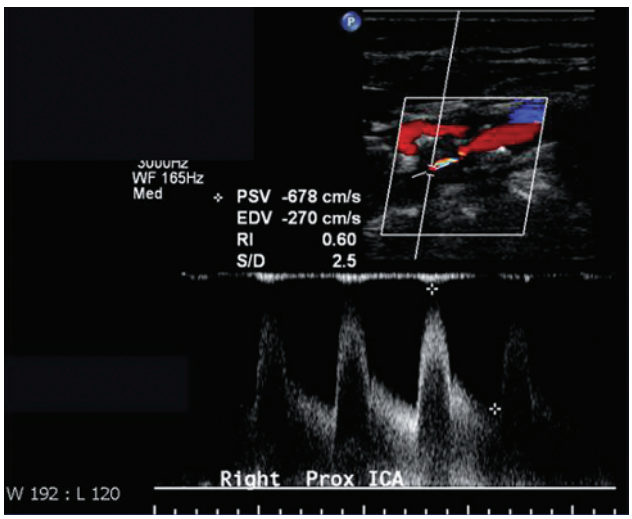

Figure 1.6 ICA waveform from the site of a >80% ICA stenosis. Both peak-systolic and end-diastolic velocities are very elevated, 678 and 270 cm/s, respectively.

Damping of spectral Doppler waveforms may be seen in the region distal to a severe carotid stenosis. The most common abnormality is spectral broadening caused by disturbed flow or turbulence. Post-stenotic flow disturbances are only qualitative measures of arterial stenosis. Post-stenotic flow disturbances that produce simultaneous forward and reverse spectral Doppler signals, accompanied by poor definition of the upper spectral border, suggest severe carotid stenosis. Severely disturbed flow distal to a stenosis may be the only indication of severe ICA stenosis when calcification prevents direct insonation of the stenosis.

Vertebral artery

The origin of the vertebral artery from the subclavian artery is by far the most common site of disease in the vertebral artery. The vertebral-artery origin lies deep in the base of the neck and may be difficult to access with ultrasound. Vertebral arteries are frequently asymmetric in size with one, most commonly the left, being larger than the other. Mean vertebral-artery diameter is about 4 mm.

The vertebral artery is most commonly interrogated with ultrasound further distally in the neck as it threads through the transverse processes of the cervical spine. Vertebral bodies are a reference to identify that it is the vertebral artery under examination (Fig. 1.7). Color Doppler is helpful to locate the vessel. The normal vertebral-artery waveform is similar to an ICA waveform. Flow in the vertebral artery is normally antegrade with a rapid upstroke and continuous diastolic flow. PSVs are reported as 20 to 40 cm/s (6), but velocities up to 80 cm/s are frequently seen without apparent clinical importance. Such velocities may represent collateral flow through a dominant vertebral artery, or a small but disease-free vertebral artery. Evaluation of disturbed flow distally may help determine if elevated velocities are associated with a vertebral-artery stenosis. Systolic and diastolic velocities may differ between two vertebral arteries if the artery diameters are asymmetric.

With high-grade subclavian-artery stenosis (subclavian steal), color flow provides an important initial clue to the diagnosis. In such cases vertebral flow is retrograde in the same direction as the vein (Fig. 1.8). Spectral Doppler will demonstrate reverse or bidirectional flow in cases of subclavian steal.

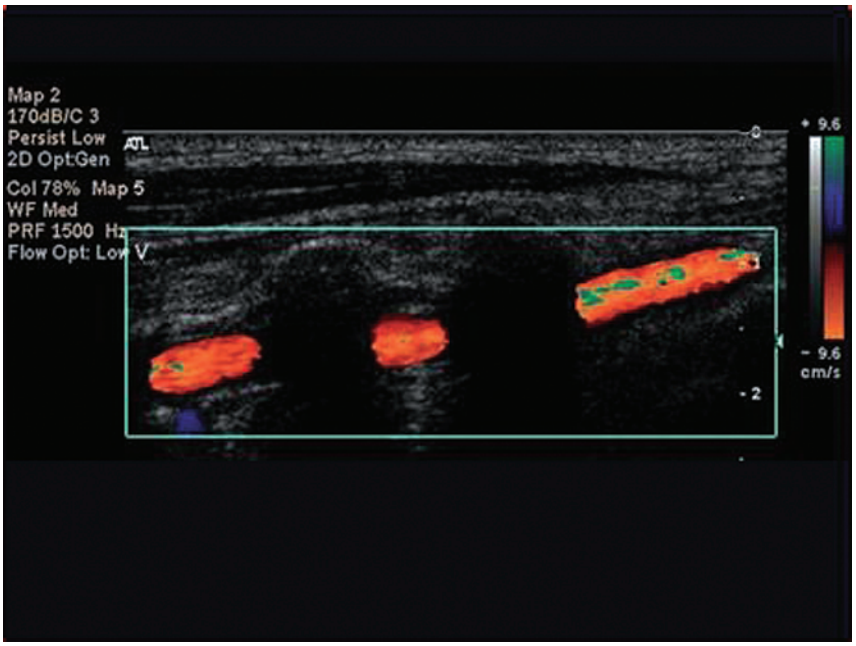

Figure 1.7 Color-flow image of a vertebral artery. Ultrasound cannot penetrate bone therefore there is no Doppler shift and no color where the artery passes through the vertebral foramen.

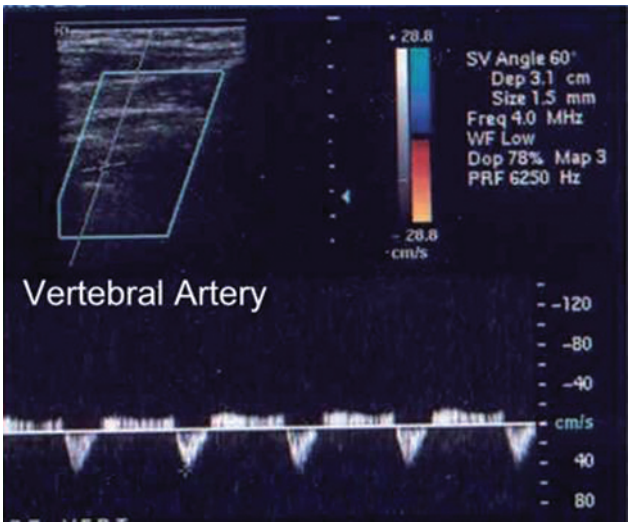

Figure 1.8 This patient has reverse flow in the vertebral artery (systolic flow below the baseline) indicating the presence of a high-grade ipsilateral subclavian-artery or inominate artery stenosis; so-called subclavian steal syndrome. In the absence of symptoms this finding is of uncertain clinical significance.

External carotid artery

The ECA is smaller in diameter than the ICA at the level of the carotid bulb, but similar in diameter beyond. It can serve as an important source of collateral flow to the brain in cases of very high-grade ICA stenosis or occlusion. In such cases the ECA may also serve as a conduit for emboli to the brain; carotid stump syndrome (7).

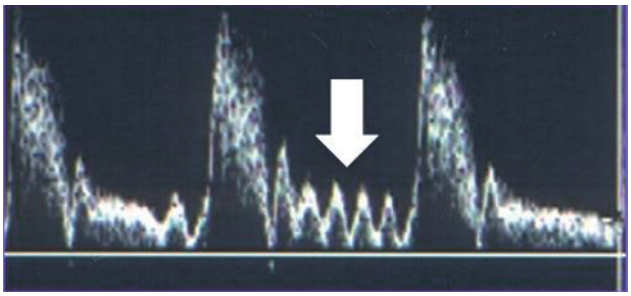

Figure 1.9 Tapping the superficial temporal artery produces reverberations (arrow) in the external carotid-artery waveform. This can sometimes help distinguish the internal from the external carotid artery during duplex-ultrasound studies of the carotid bifurcation.

The ECA waveform has a sharp upstroke, a prominent dichrotic wave in late systole or early diastole, and a velocity waveform that is near or at the zero baseline at end diastole. The PSV of the ECA is normally higher than the ICA. The ECA may adopt the characteristics of the ICA in end diastole if the resistance in the face and scalp decreases with temperature change and/or in the presence of disease. Tapping the superficial temporal artery can cause reverberations in the ECA that can serve as an aid to identifying the ECA during carotid duplex-ultrasound studies (Fig. 1.9).

Classifying carotid stenosis

Duplex-derived categories of stenosis are relatively broad and were developed by comparing duplex-derived spectral

waveforms and contrast arteriograms. Sensitivities and specificities for detecting an ICA stenosis of >50% to 99% are between 90 and 95%. Numerous criteria exist for classifying ICA stenosis. Some focus on categories of stenosis, others focus on threshold levels of stenosis.

One of the most widely accepted classification schemes for categories of ICA stenosis was developed at the University of Washington. In this classification scheme waveform analysis was used to classify ICA angiographic stenosis as normal, 1–15%, 16–49%, 50–79%, 80–99% stenosis, and occlusion. Prospective validation has demonstrated an overall agreement of 82% with angiography. The ability of the criteria to detect carotid disease is 99% sensitive. The ability of the criteria to recognize normal arteries is 84% specific (3).

Criteria for detecting carotid-artery stenosis scanning underwent re-evaluation stimulated by randomized trials that took place over two decades, testing the efficacy of carotid endarterectomy (CEA) (8–12). The trials identified benefits in stroke reduction for CEA in patients with specific levels of ICA stenosis. Patients with symptomatic ICA stenosis >70% upto 99% benefited dramatically from CEA. Patients with symptomatic ICA stenosis between 50% and 69%, and patients with asymptomatic ICA stenosis between 60% and 99% also benefited from CEA but to a lesser extent.

In North American trials, ICA stenosis was calculated from arteriograms by comparing the diameter of the minimal residual lumen with the diameter of the distal cervical ICA (13). The University of Washington criteria pre-existed the CEA trials, and were developed comparing the residual ICA lumen at its narrowest point with an estimate of the ICA bulb diameter. The bulb has a greater diameter than the distal ICA, so the two methods do not give the same calculated percentage angiographic stenosis for the same lesion. Calculations using the distal ICA as the reference vessel provide lower calculated stenosis percentages than calculations using the bulb as the reference site. This effect is particularly striking for modest lesions (14), and therefore duplex criteria for ICA stenosis using the bulb as the reference vessel are not directly applicable to the results of the randomized trials establishing benefit of CEA.

Current Criteria for internal carotid-artery stenosis

New criteria for ICA stenosis have been developed comparing duplex scans with angiographic ICA stenosis using the distal ICA as the reference vessel in calculating angiographic stenosis. Such criteria are useful for selection of patients for carotid intervention because they are directly applicable to the threshold levels of carotid stenosis addressed in the CEA trials. The initial studies were performed at the Oregon Health & Science University (OHSU) (5,15). Subsequent publications proposed different criteria for the identification of clinically relevant threshold levels of ICA stenosis (16–21).

Given the proliferation of different criteria for ICA stenosis, a panel from a variety of medical specialties assembled to review the carotid ultrasound literature. The panel developed a consensus statement regarding the key components of the carotid ultrasound examination and reasonable criteria for stratification of ICA stenosis (22). They recommended carotid examinations be performed with gray-scale imaging, color, and spectral Doppler. Doppler waveforms should be obtained with a Doppler angle close to but not exceeding 60°. The panelists recommended broad diagnostic strata to estimate ICA stenosis. The panel also concluded Doppler is relatively inaccurate for subcategorizing ICA stenoses <50%, and recommended that these lesions be reported under a single category, as <50% stenosis.

The consensus panel recommended PSV as the primary diagnostic parameter but noted that data suggested reproducibility of PSV has sufficient problems such that it should not be considered a continuous variable for classifying carotid stenosis. The degree of stenosis estimated by ICA PSV and the degree of narrowing of the ICA lumen seen on gray scale and color Doppler should also correlate with PSV. Additional parameters, such as the ICA/CCA PSV ratio and ICA EDV, were recommended as secondary parameters that are useful when ICA PSV may not be representative of the extent of disease. The consensus panel recommended criteria that stratified ICA stenosis into specific categories relevant to the CEA trials (Table 1.1).

Bilateral high-grade internal carotid-artery stenosis

Doppler-derived flow velocities from the ICA opposite an ICA occlusion or high-grade stenosis may suggest a higher degree of narrowing than observed angiographically, likely as a result of compensatory flow (2). Duplex-scan overestimation of stenosis is more common in less-severe categories of stenosis than in higher-severity categories (23).

Stented carotid arteries

Stents in the carotid artery are generally easily visible on gray-scale and color imaging (Fig. 1.10). Ultrasound criteria developed for native ICAs are likely not applicable to stented carotid arteries, especially for modest lesions in stented ICAs. The number of patients in studies of stented carotid arteries that have actually had severe in-stent restenosis is small. No study has yet correlated stenosis within a stented carotid artery with clinical symptoms or outcomes. Currently it appears that for more modest lesions higher PSVs, >125 cm/s, will be needed to identify a >50% stenosis in a stented

Table 1.1 Consensus Panel Recommendations for Classification of Internal Carotid-Artery Stenosis. With permission from Grant *et al.* (22)

Classification	Recommendation
Normal	The ICA PSV is less than 125 cm/s and there is no visible plaque or intimal thickening. Normal arteries should also have an ICA/CCA ratio of less than 2.0 and ICA EDV of less than 40 cm/s
ICA stenosis <50%	Present when the ICA PSV is less than 125 cm/s and there is visible plaque or intimal thickening. Such arteries should also have an ICA/CCA PSV ratio of less than 2.0 and an ICA EDV of less than 40 cm/s
ICA stenosis of 50–69%	Present when the ICA PSV is 125–230 cm/s and there is visible plaque. Such arteries should also have an ICA/CCA PSV ratio of 2.0–4.0 and an ICA EDV of 40–100 cm/s
ICA stenosis of ≥70–99%	Less than near occlusion is present when the ICA PSV is more than 230 cm/s and there is visible plaque with lumen narrowing on gray-scale and color Doppler imaging. The higher the PSV, the more likely (higher positive predictive value) it is to have severe disease. Such stenoses should also have an ICA/CCA ratio of more than 4.0 and an ICA EDV of more than 100 cm/s
Near occlusion of the ICA	Velocity parameters may not apply. "Pre-occlusive" lesions may be associated with high, low, or undetectable velocity measurements. The diagnosis of near occlusion is therefore established primarily by demonstration of a markedly narrowed lumen with color Doppler. In some near occlusive lesions, color Doppler can distinguish between near occlusion and occlusion by demonstrating a thin wisp of color traversing the lesion
Occlusion	There is no detectable patent lumen on gray-scale imaging and no flow with spectral, color, and power Doppler. Near occlusive lesions may be misdiagnosed as occlusions when only gray-scale ultrasound and spectral Doppler are used

CCA, common carotid artery; ICA, internal carotid artery; EDV, end-diastolic velocity; PSV, peak-systolic velocity.

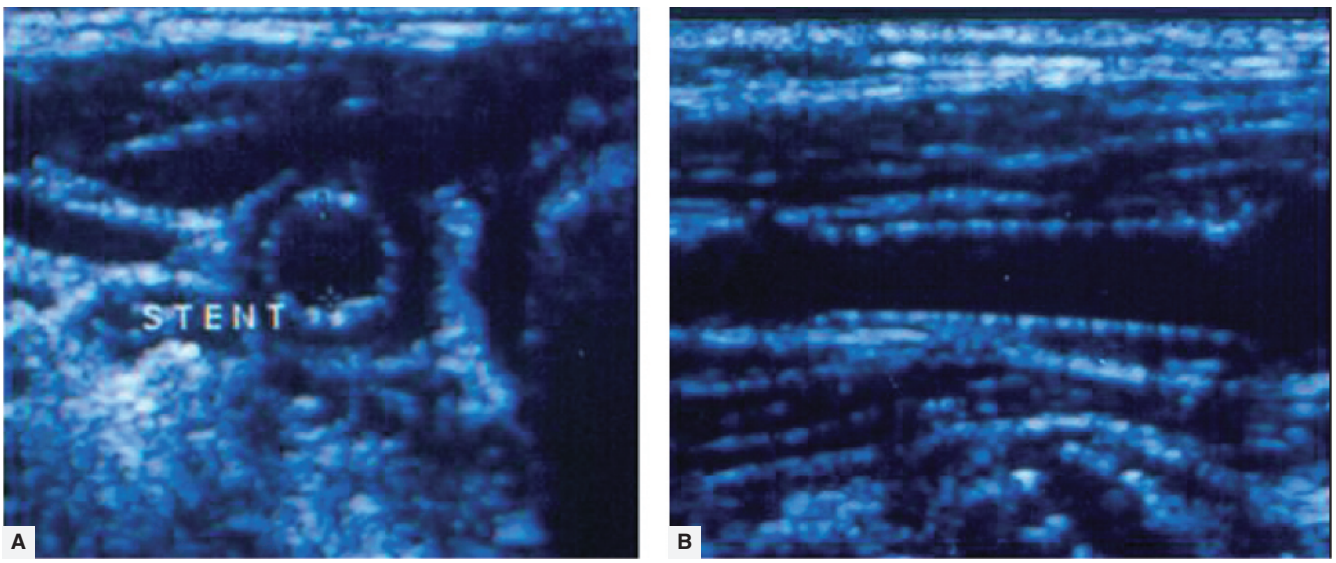

Figure 1.10 **(A)** Cross-section and **(B)** longitudinal gray-scale images of an internal carotid-artery stent.

ICA. Criteria to detect high-grade stenosis in native ICAs still work reasonably well to identify high-grade stenosis in stented ICAs (24).

External carotid-artery and common carotid-artery stenosis

As with the ICA, relative degrees of stenosis in the ECA and CCA may be determined by the presence of plaque with B-mode imaging, aberration in color flow on duplex examination, spectral broadening, and increases in PSV. Although not specifically tested, stenosis of more than 50% can be inferred by the presence of a focally increased PSV followed by post-stenotic turbulence. As noted above the CCA waveform normally has attributes of the ICA and ECA. The CCA will take on the quality of the "normal" vessel (ICA or ECA) when the other is occluded. If there is a proximal CCA (or innominate

artery) high-grade stenosis or occlusion, the ipsilateral CCA Doppler waveform will be dampened with low PSVs when compared with the contralateral side. Post-stenotic turbulence may be present. There are no widely employed and validated duplex criteria to estimate diameter reductions in the CCA or ECA. Stenosis of >50% has generally been inferred by PSV >125 cm/sec associated with post-stenotic turbulence. However, one study using computed tomographic angiography as the reference standard suggested, at least for the CCA, a PSV of >180 cm was best for distinguishing a <50% from a >50% CCA stenosis (sensitivity 64%, specificity 88%) (25).

Miscellaneous carotid conditions

Carotid duplex ultrasound can be an aid to diagnosis of a number of other conditions affecting the carotid artery other than atherosclerotic stenotic lesions. Fibromuscular disease can be often recognized in the mid-to-distal cervical ICA as a "string of beads" image on power Doppler (Fig. 1.11). Carotid dissection can be recognized by the presence of visible flaps on gray-scale imaging and to-and-fro flow in the ICA (Fig. 1.12). Carotid aneurysms (Fig. 1.13) and carotid-body tumors (Fig. 1.14) also have distinct appearances on carotid duplex scanning.

Peripheral artery duplex scanning

Lower-extremity arteries

Duplex scanning can provide detailed anatomic and hemodynamic information from the infrarenal aorta to the distal tibial vessels. Arterial duplex scanning has been prospectively compared with angiography to establish standard criteria for normal and diseased arteries (26). Sensitivity of duplex examination for detecting the presence of a hemodynamically important lesion (>50%) ranges from 89% at the iliac artery to 68% at the popliteal artery. Overall sensitivities for predicting interruption of patency are 90% for the anterior and posterior tibial arteries, and 82% for the peroneal artery. The technique is versatile and does not appear to be heavily influenced by the presence of previous operations or multilevel disease (Fig. 1.15).

Velocity patterns and classification of percent stenosis

Extremity duplex-derived arterial waveforms from normal resting peripheral arteries are triphasic with end-diastolic flow near zero, reflecting high resistance associated with peripheral arteries (Fig. 1.16). Triphasic

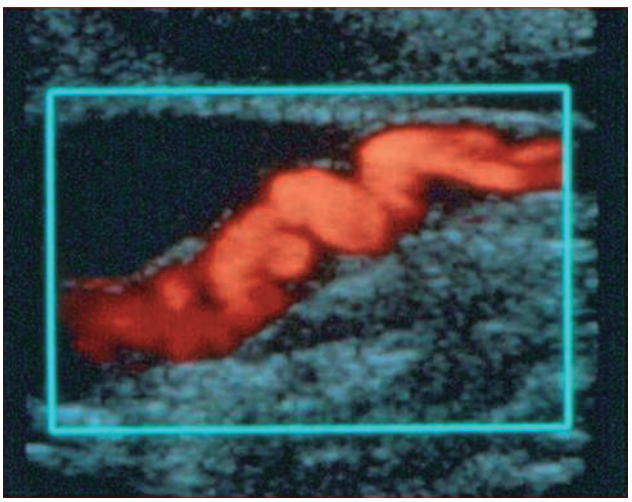

Figure 1.11 Power Doppler image of an internal carotid artery with fibromuscular disease. The classic "string of beads" appearance was easily recognized in this patient.

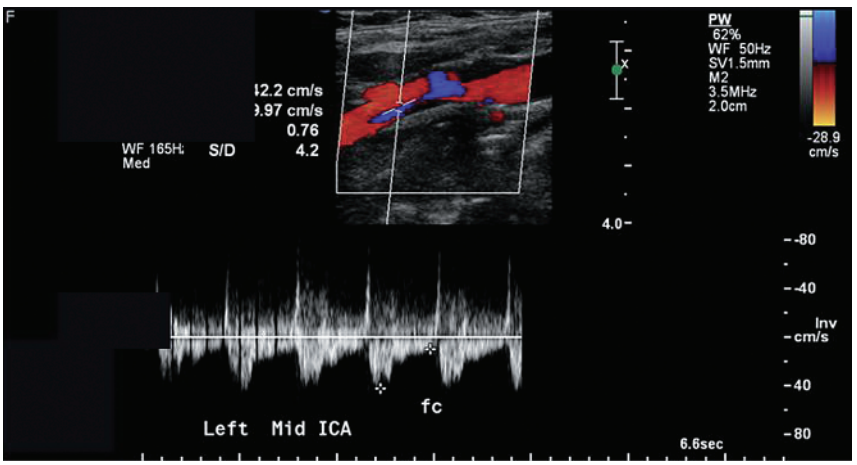

Figure 1.12 Typical internal carotid-artery flow pattern in a patient with carotid-artery dissection. The to-and-fro flow pattern results in obstruction of flow in the false lumen distally.

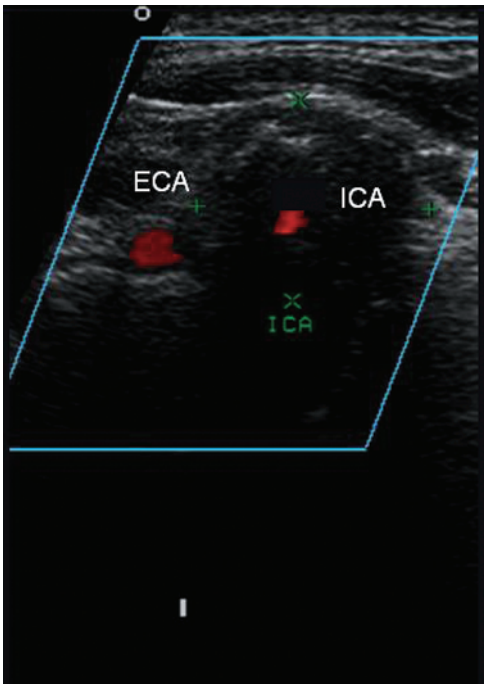

Figure 1.13 Cross-sectional image of an internal carotid aneurysm. There is minimal residual lumen of the internal carotid artery as a result of laminated thrombosis in the aneurysm. The aneurysm was replaced with a vein graft.

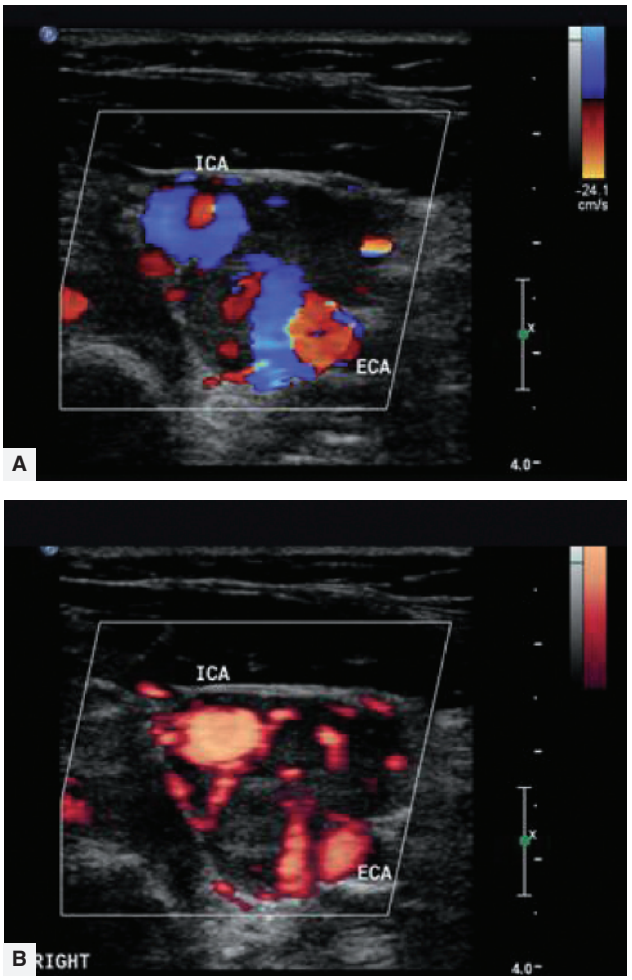

Figure 1.14 **(A)** Color and **(B)** power Doppler images of a carotid-body tumor. The tumor splays the carotid bifurcation, and the color flashes within the tumor reflect the highly vascular nature of these tumors.

waveforms are maintained from the aorta to the ankle. PSV decreases from the iliac arteries to the tibial arteries. PSVs are similar in the three tibial arteries in normal subjects.

Changes in the velocity waveforms indicating disease include absence of end-systolic reverse flow and elevation of PSV. The University of Washington criteria for classification of peripheral arterial stenoses are shown in Table 1.2 (27).

Peak-systolic-velocity ratios, comparing the PSV within the stenosis to the PSV just proximal to the stenosis, are also useful for grading stenosis and are highly reproducible (28,29). Fifty percent stenoses in lower-extremity arteries correlate with PSV ratios from 1.4 to 3.0 (26, 30–33). A velocity ratio of 2.0 is a reasonable compromise and is used by many vascular laboratories as indicative of a 50% peripheral arterial stenosis.

Lower-extremity duplex scanning can serve as an alternative to contrast arteriography in the preoperative assessment of selected patients for intervention. Successful lower-extremity revascularization by bypass grafting or catheter-based techniques has been reported using only arterial duplex (34–36). The limiting factor is identification of the best site for the distal anastomosis of a bypass graft, especially below the knee (37). Most centers continue to employ other forms of imaging to supplement duplex scanning prior to intervention for peripheral arterial disease.

Duplex-ultrasound scanning plays a key role in the postoperative assessment and follow-up of lower-extremity vein grafts. Detection and repair of graft-threatening stenoses detected by duplex scanning appears to improve secondary graft patency (38–41). Twenty to thirty percent of vein grafts will develop a severe-enough stenosis that revision is recommended. Surveillance is recommended for the life of the graft (42). A widely utilized protocol for vein-graft duplex surveillance is every 3 months for the first year, and every 6 months thereafter.

The examination involves insonation of the proximal inflow artery, proximal anastomosis, mid-graft, distal anastomosis, and the distal outflow artery (Fig. 1.16). A PSV ratio of four, or a PSV above 300 cm/s, indicates a critical graft stenosis where repair of the lesion should be considered (43) (Fig. 1.17). When the PSV ratio is between two and four, the patient should be re-evaluated in 3 months with a duplex examination.

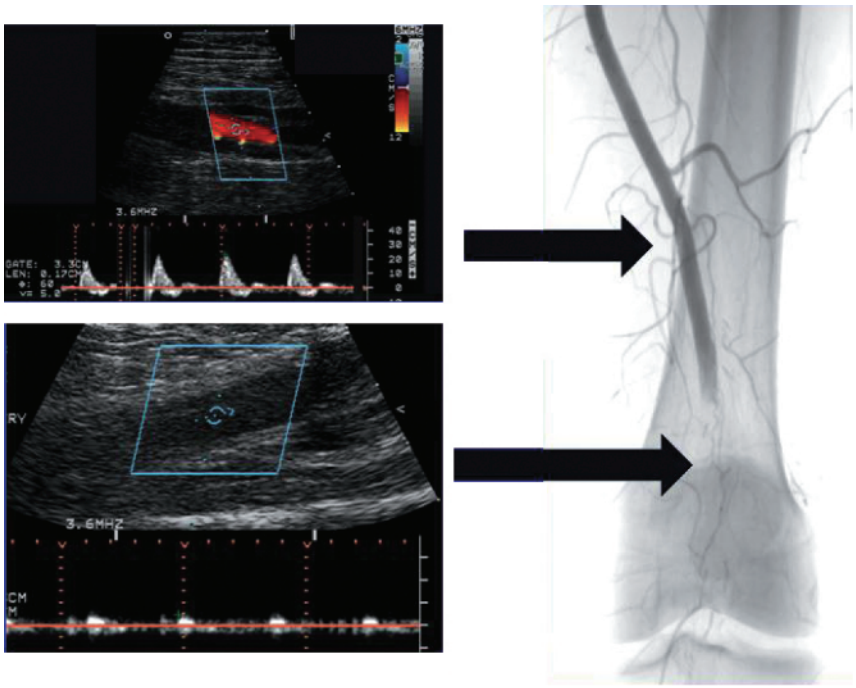

Figure 1.15 Duplex waveforms and a corresponding angiogram in a patient with acute lower-extremity ischemia. There is no detected flow in the area of angiographically confirmed popliteal-artery occlusion.

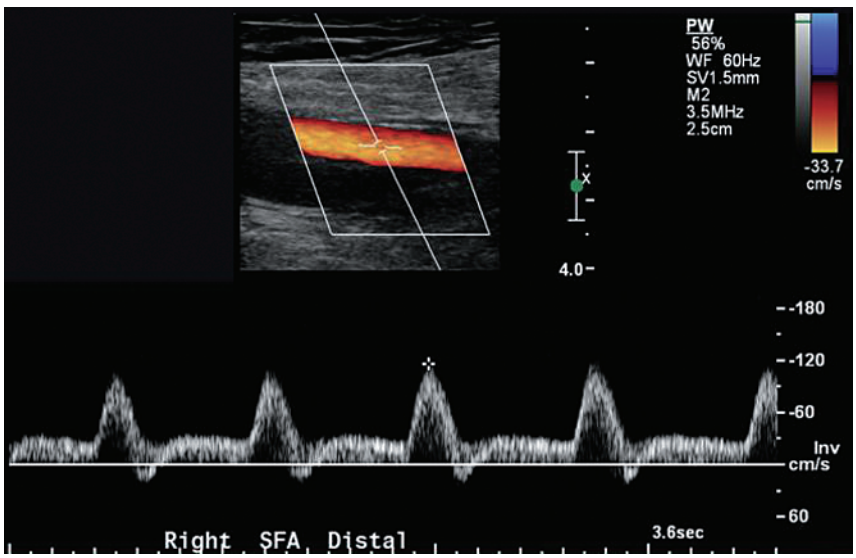

Figure 1.16 Color-flow image and normal triphasic waveform from a non-diseased superficial femoral artery.

Table 1.2 University of Washington Duplex Criteria for Determination of Stenosis in Lower-extremity Arteries

Degree of stenosis (%)	Duplex-ultrasound criteria
0	Normal waveform and velocities
1–19	Normal waveform and velocities with spectral broadening
20–49	Marked spectral broadening, 30% increase in PSV
50–99	Marked spectral broadening, 100% increase in PSV Loss of reverse-flow component of waveform
Occluded	No detectable flow signal in well-visualized artery

PSV, peak systolic velocity.

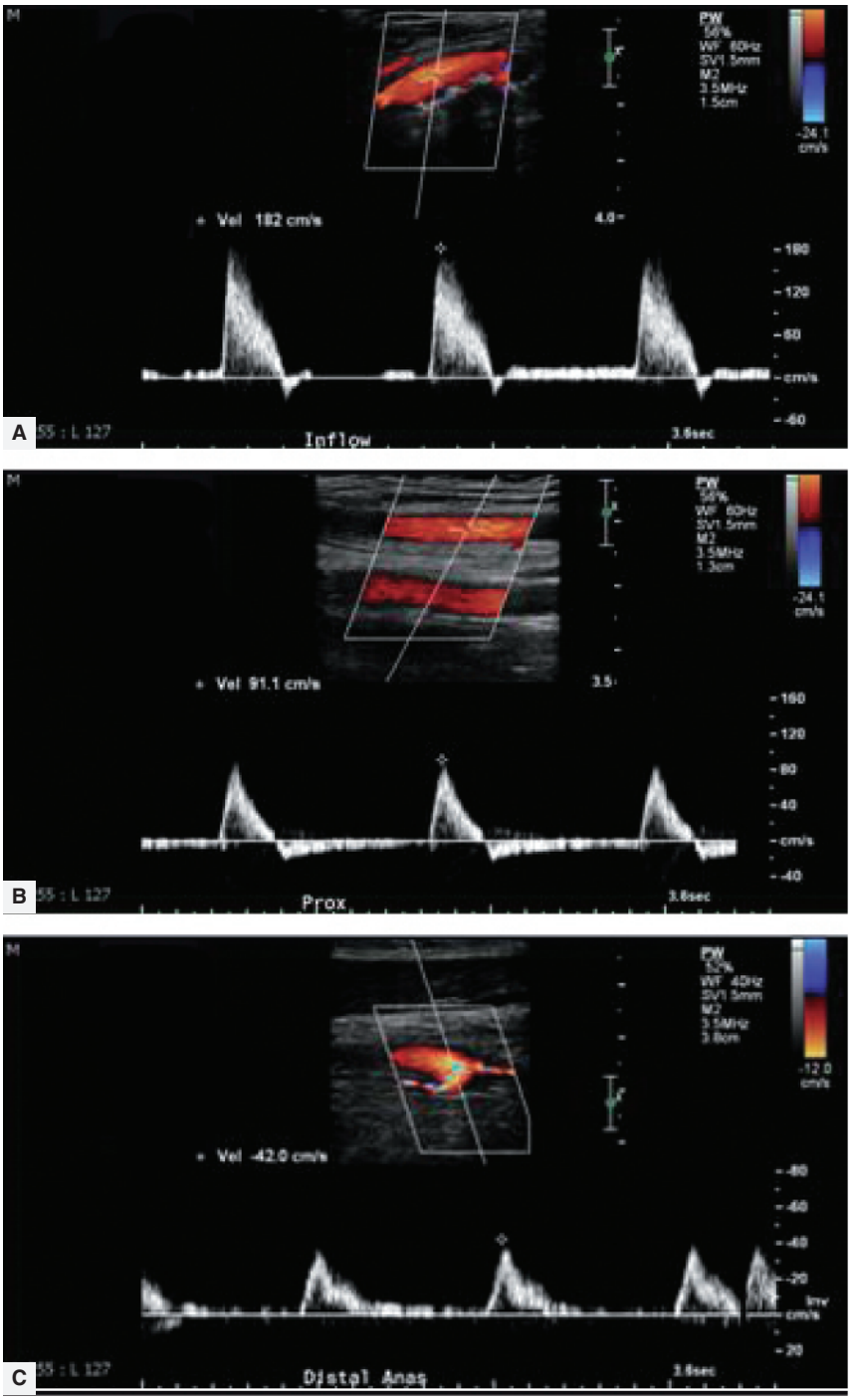

Figure 1.17 Duplex examination of the common femoral artery **(A)** proximal to a lower-extremity bypass, the proximal portion of the bypass and **(B)** the distal anastomotic site of the bypass. The common femoral artery exhibits a normal triphasic waveform, and distal velocities are within normal ranges for a lower-extremity bypass graft. Vein grafts must be examined along their entire length in a point-to-point fashion to exclude areas of focal stenosis.

Upper-extremity arteries

Upper-extremity arterial disease is a small but important component of vascular surgical practice. In the upper extremity, plethysmographic techniques are probably more important than duplex scanning, but duplex still can play a significant role in the evaluation of upper-extremity arterial disease.

Duplex scanning of the upper extremity is carried out in a manner similar to arterial examination elsewhere.

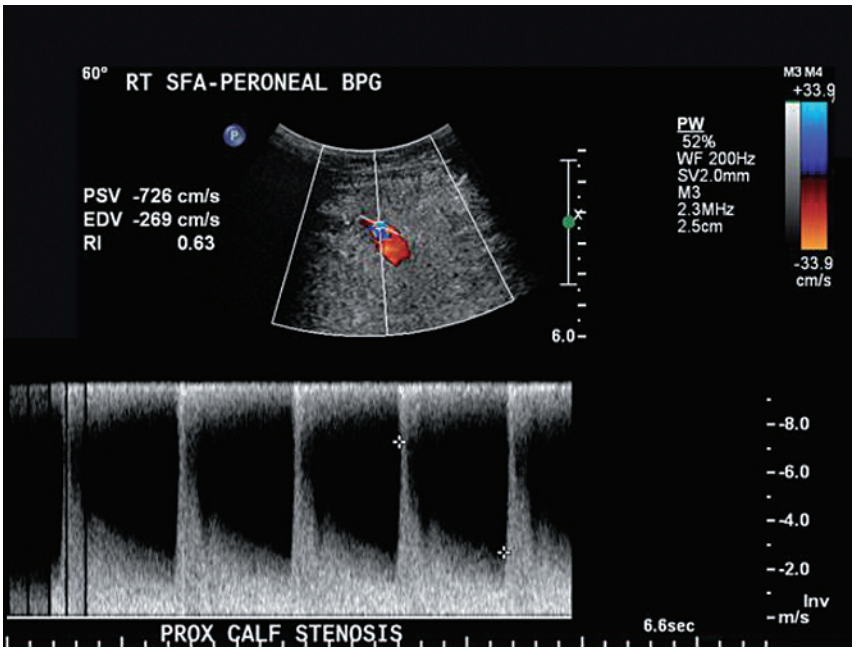

Figure 1.18 A peak-systolic velocity (PSV) of over 700 cm/sec indicates a high-grade stenosis in the femoral to peroneal-artery vein-bypass graft.

The origins of the brachial cephalic vessels can be difficult to visualize with duplex scanning. For examination of the origin of the subclavian artery a 3 or 5 MHz transducer, with a small footprint probe using the sternal notch as a window, generally gives the best images. A recent study found 48 of 50 right subclavian-artery origins (96%), and 25 (50%) of 50 left subclavian-artery origins could be visualized by color duplex scanning (44) (Fig. 1.18).

Criteria for stenosis at the origins of brachial cephalic arteries are slightly different than those used elsewhere. Such criteria are necessary for origins of the brachiocephalic vessels. If only PSV ratios are utilized there would be higher numbers of both false-positive and false-negative results (44).

A PSV ratio of greater than two indicates stenosis at the origin of a brachial cephalic artery. Monophasic flow without actual visualization of a high-velocity jet also implies significant stenosis, as does reverse flow in a vertebral artery. Distally upper-extremity arteries are fairly superficial and generally constant in location. They are best scanned with high-frequency transducers (7.5 or 10 MHz). Color facilitates identification of the vessels (Fig. 1.19).

Interpretation of duplex findings of upper-extremity arteries beyond their origins is similar to lower-extremity arteries (45). Waveforms are normally triphasic. Stenoses will produce high-velocity jets, post-stenotic turbulence, and dampened distal waveforms. There are, however, at present no specific criteria to gauge severity of arterial stenoses in the upper extremity. Guidelines are listed in Table 1.3.

Duplex scanning is quite useful for patients with unilateral symptoms who may have a surgically correctable problem (46) (Figs 1.20–1.22). Duplex evaluation of upper-extremity aneurysms is based on B-mode imaging. The most important features are the diameter and location of the enlarged artery and the presence of intraluminal thrombsis, that may serve as a potential embolic source. Flow within the aneurysm can be determined by Doppler.

Whereas duplex scanning alone cannot be used to make the diagnosis of Takayasu's arteritis, it can be a helpful adjunct in following the progression or regression of arterial involvement in response to treatment (47).

Visceral arteries

Mesenteric arteries

Duplex ultrasonography is a valuable screening test for splanchnic-artery stenosis in patients with possible chronic mesenteric ischemia. It can also be used for follow-up of mesenteric-artery reconstructions. Chronic mesenteric ischemia is a clinical diagnosis. Angiographic confirmation of high-grade stenoses or occlusion of the splanchnic vessels, and an appropriate history and physical examination are required for a final diagnosis of chronic mesenteric ischemia.

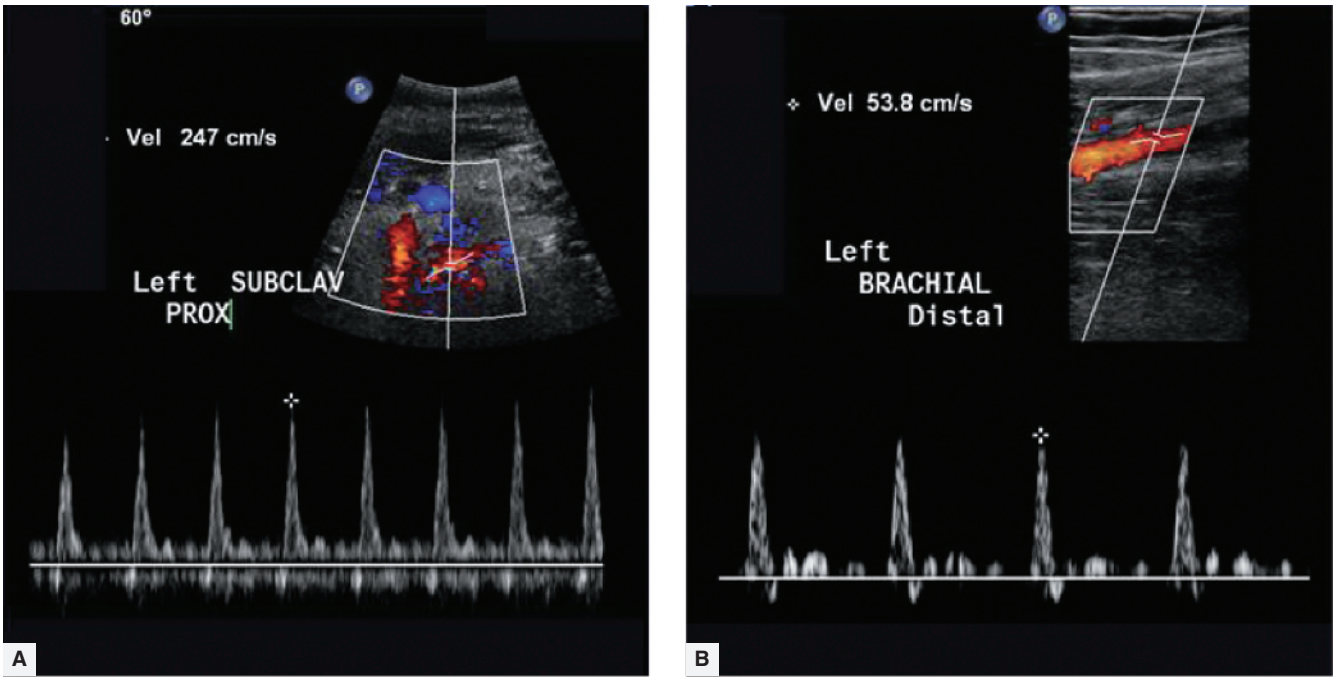

Figure 1.19 A PSV of 247 cm/s **(A)** suggests stenosis in the proximal subclavian artery. In this case the ipsilateral brachial artery had a normal velocity and a normal triphasic waveform **(B)** suggesting the subclavian lesion is unlikely to be pressure reducing.

Table 1.3 Duplex-Ultrasound Criteria for Evaluation of Upper-extremity Arterial Stenosis

Condition	Characteristics
Normal	Uniform waveforms; biphasic or triphasic waveforms; clear window beneath systolic peak
<50% diameter reduction	Focal velocity increase; spectral broadening; possibly triphasic or biphasic flow
>50% diameter reduction	Focal velocity increase; loss of triphasic or biphasic velocity waveform; post-stenotic flow (color bruit)
Occlusion	No flow detected

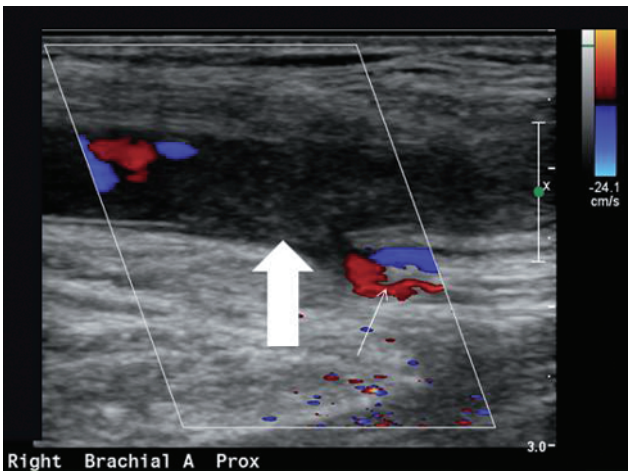

Figure 1.20 The image demonstrates abrupt occlusion of the brachial artery (large arrow) at the site of a collateral vessel (small arrow).

Ultrasound examination of splanchnic arteries is technically difficult and best performed by those with extensive experience in intra-abdominal ultrasound techniques. Examination is generally confined to the celiac and superior mesenteric arteries, although the inferior mesenteric artery can often be visualized as well. Mesenteric duplex is not particularly useful in patients with acute mesenteric ischemia as bowel gas frequently obscures the mesenteric vessels.

Interpretation of mesenteric duplex-ultrasound studies

Velocity waveforms differ in the superior mesenteric artery (SMA) versus the carotid artery (CA). The liver and spleen have high constant metabolic requirements and are low-resistance organs. As a result, CA waveforms are generally biphasic, with a peak-systolic component, no reversal of end-systolic flow, and a relatively high end-diastolic flow. The fasting SMA velocity waveform is often triphasic. There is a peak-systolic component, often an end-systolic reverse-flow component, and a minimal diastolic flow component (48) (Fig. 1.23A).

Changes in splanchnic-artery waveforms with feeding differ in the CA and SMA. There is no significant

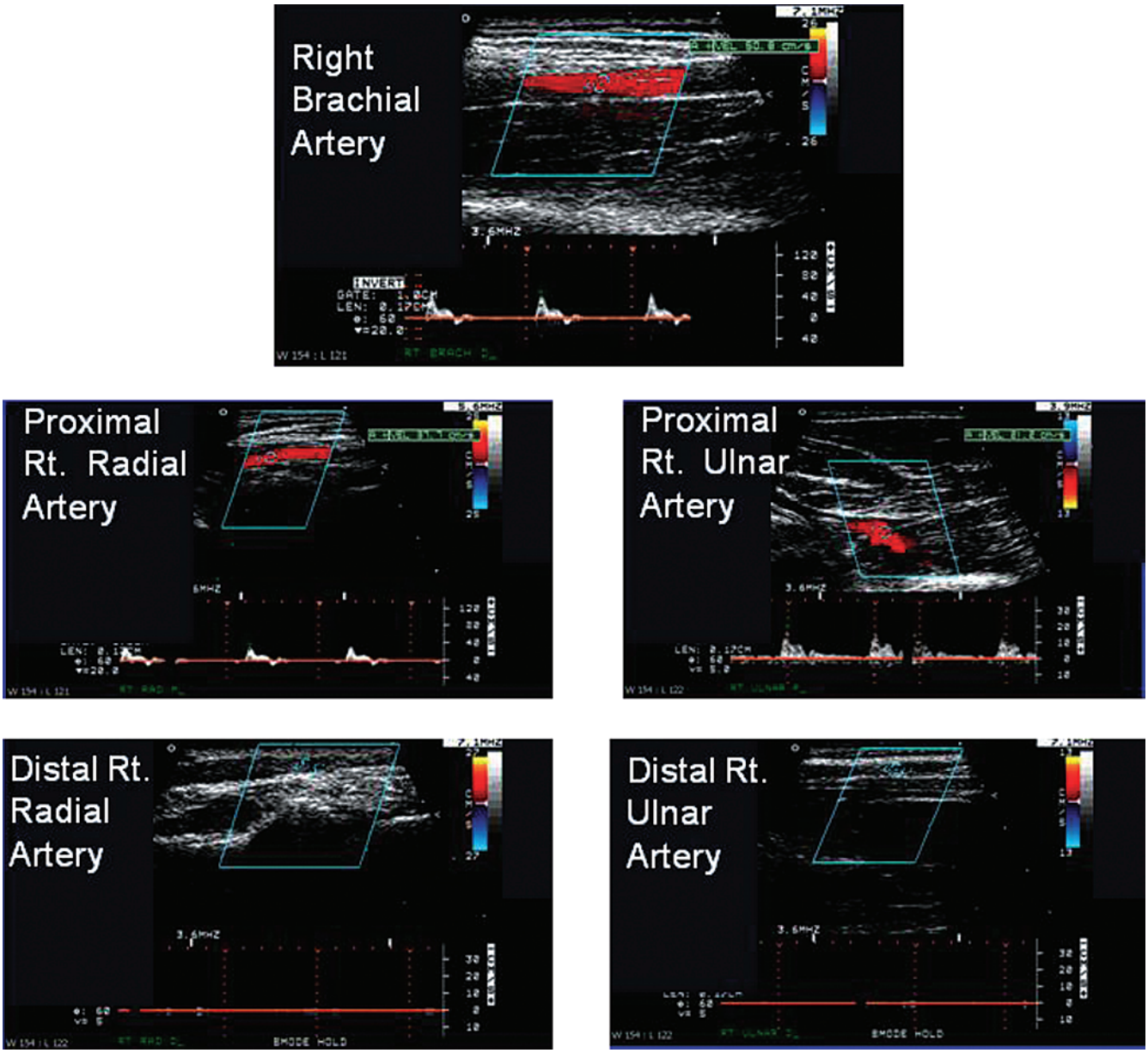

Figure 1.21 The distal radial and ulnar arteries are occluded in this patient with chronic embolization secondary to a subclavian-artery aneurysm associated with a cervical rib.

change in CA velocity waveform after eating. However, SMA blood flow increases dramatically after a meal in response to a decrease in intestinal arterial resistance. There is a near doubling of systolic velocity, tripling of the EDV, and loss of end-systolic reversal of blood flow (49) (Fig. 1.23B). Changes are maximal at 30 to 45 min after eating. Mixed-composition meals produce the greatest flow increase in the SMA when compared with equal caloric meals composed solely of fat, glucose, or protein (50).

Detection of splanchnic arterial stenosis

Duplex ultrasound can detect hemodynamically significant stenoses in the main mesenteric arteries. In a blinded prospective study of 100 patients who underwent mesenteric-artery duplex scanning and lateral aortography, a PSV in the SMA of 275 cm/s or more indicated a ≥70% SMA stenosis, with a sensitivity of 92%, a specificity of 96%, a positive predictive value of 80%, a negative predictive value of 99%, and an accuracy of

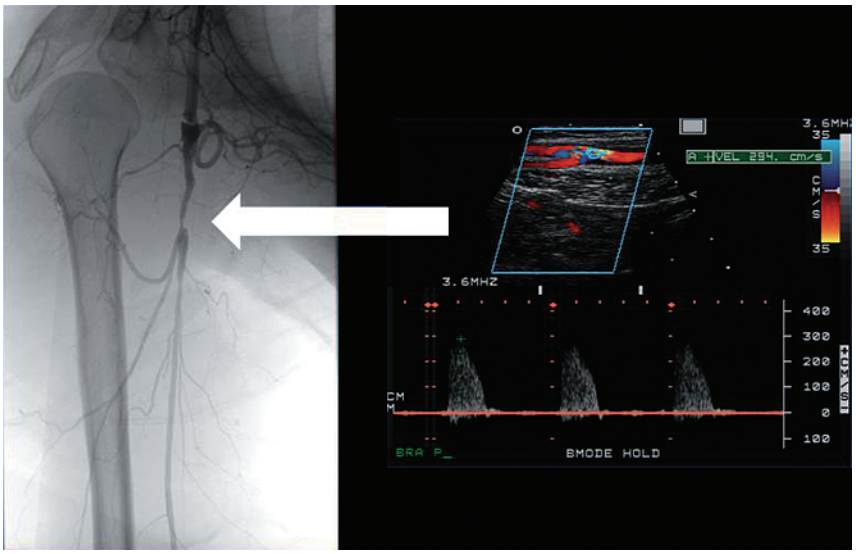

Figure 1.22 Duplex color-flow image and velocity waveform, and corresponding angiogram in a patient with brachial artery stenosis and symptomatic arm ischemia secondary to a crutch injury.

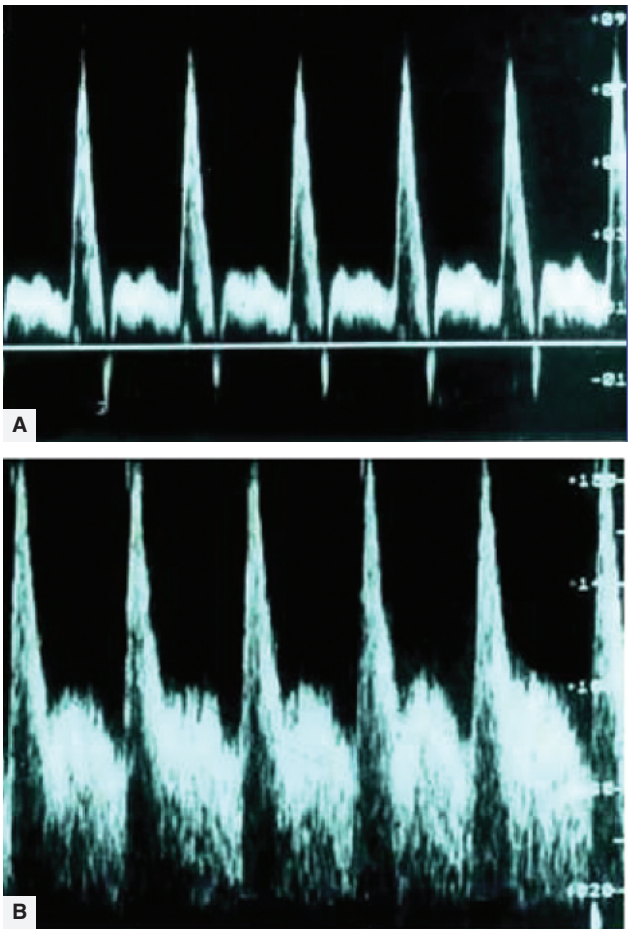

Figure 1.23 **(A)** A normal fasting superior mesenteric-artery (SMA) waveform may exhibit reverse flow at the end of systole and relatively low-end diastolic velocity reflecting relatively high resistance of the intestinal circulation in the fasting state. **(B)** Postprandial SMA waveform. There has been, in comparison with (A), loss of end-systolic reverse flow and an increase in end-diastolic flow as resistance in the intestinal arterial circulation falls following feeding.

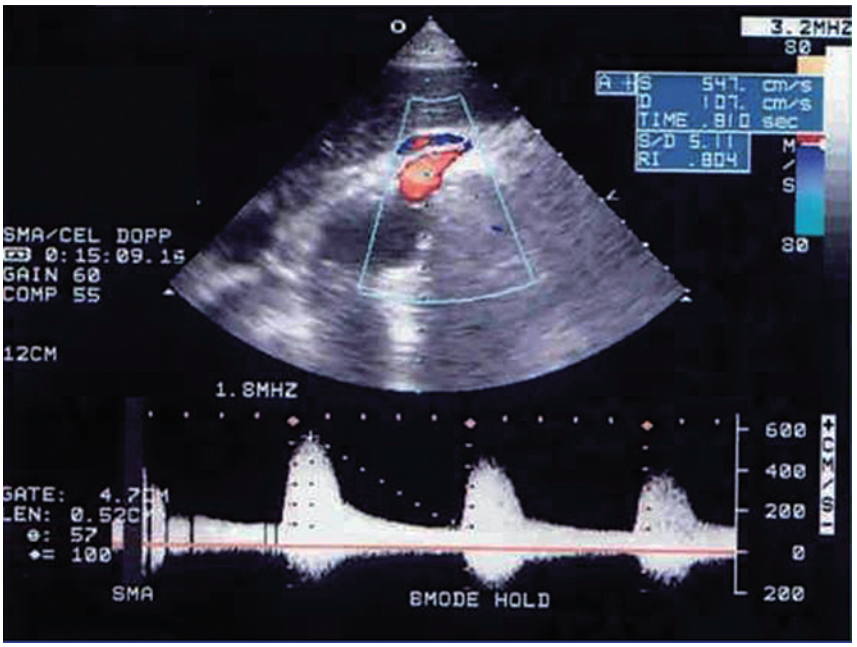

Figure 1.24 Color-flow image and duplex-derived SMA waveform in a patient with chronic mesenteric ischemia. A PSV of 547 cm/s indicates a high-grade SMA stenosis and is compatible with the clinical diagnosis of chronic mesenteric ischemia.

96% (Fig. 1.24). In the same study, a PSV of ≥200 cm/s identified a ≥70% angiographic celiac artery stenosis, with a sensitivity of 87%, a specificity of 80%, a positive predictive value of 63%, a negative predictive value of 94%, and an accuracy of 82% (51).

There are other duplex criteria for splanchnic-artery stenosis. An SMA EDV >45 cm/s correlates with a ≥50% SMA stenosis, with a specificity of 92%, and a sensitivity of 100%, whereas a CA EDV of >55 cm/s predicts a ≥50% CA stenosis, with a sensitivity of 93%, specificity of 100%, and accuracy of 95% (52).

Surgical bypass can be used to treat mesenteric ischemia. Mesenteric-artery bypass grafts can be followed postoperatively with mesenteric-artery duplex scanning (Fig. 1.25). Flow velocities within mesenteric-artery bypass grafts vary little with the origin of the graft (supreceliac or infrarenal aorta, or a common iliac artery) and remain stable over time. Serially increasing velocities over time in a mesenteric bypass likely suggest the development of a graft or anastomotic stenosis (53).

Placement of an intraluminal stent is an alternative to surgical bypass in the treatment of mesenteric-artery stenosis. There is reason to suspect duplex criteria developed for stenosis in native mesenteric arteries may not be applicable to stented superior mesenteric arteries. To date a single study has examined this issue. Mesenteric duplex scans pre and post placement of a SMA stent were compared and correlated with pressure gradients measured at the time of angiography. The data indicated SMA stenting provides good anatomic results and significantly reduces pressure gradients. Duplex-measured SMA PSVs are reduced post-stenting but, despite good angiographic results, seem to remain above levels predicting high-grade native artery SMA stenosis (54).

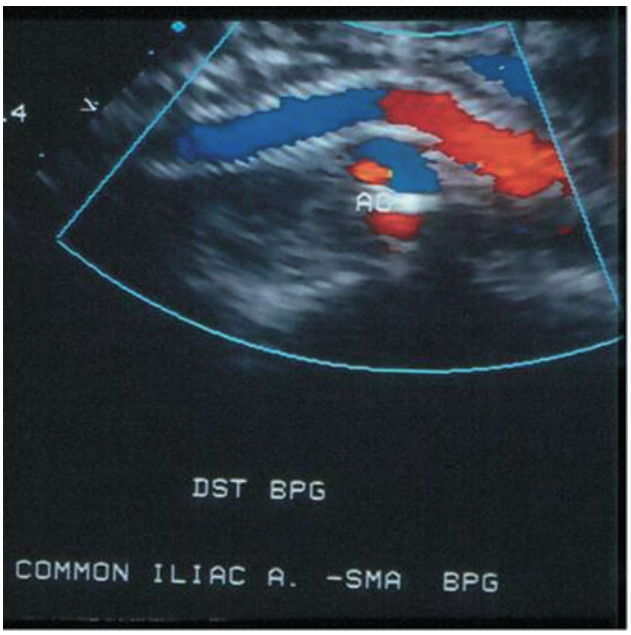

Figure 1.25 Color-flow image of a common iliac-to-SMA bypass graft.

Renal arteries

Indirect assessment of renal-artery stenosis

Main renal-artery stenosis can be evaluated indirectly by assessment of interlobar arteries. Decreased acceleration times and tardus/parvus waveforms (waveforms with delayed or slowed upstrokes) suggest a main renal-artery stenosis. Indirect examination is easier to perform than direct examination of the main renal arteries. Indirect techniques are less accurate in patients with bilateral stenoses and are not applicable in patients with a single patent renal artery. In addition, indirect techniques have not been widely validated, and improved visualization of main renal arteries with modern duplex scanners has made them basically obsolete.

Direct assessment of renal-artery stenosis

Normal renal arteries have a PSV less than 180 cm/s and low-resistance waveforms reflecting the high metabolic demands of the kidney (Fig. 1.26). A ratio of the PSV in the renal artery to that in the aorta (renal aortic ratio, RAR) of ≥3.5 indicates a ≥60% diameter-reducing renal-artery stenosis (84 to 88% sensitivity, 97 to 99% specificity, 94 to 98% positive predictive value) (55). A PSV of ≥200 cm/sec has also been suggested to indicate a ≥60% renal-artery stenosis, whereas a velocity in the renal artery of > 185 cm/s has been suggested to indicate a renal-artery stenosis of <60% (Fig. 1.27). Therefore, a renal artery can be considered normal when PSV is <180 cm/s and the RAR is <3.5. With a PSV >180 cm/s and a RAR <3.5, the renal artery can be considered to have a <60% stenosis. RARs of >3.5 indicate >60% renal-artery stenosis, regardless if the renal-artery PSV is less than or more than 180 cm/s (56). When the EDV is >150 cm/sec, data suggest a >80% renal-artery stenosis (57). The same criteria have been used to evaluate the patency of renal arterial reconstructions but may need modification for stented renal arteies (58).

Predicting success of renal-artery interventions

In patients with renal insufficiency EDVs tend to be lower, suggesting increased parenchymal resistance to

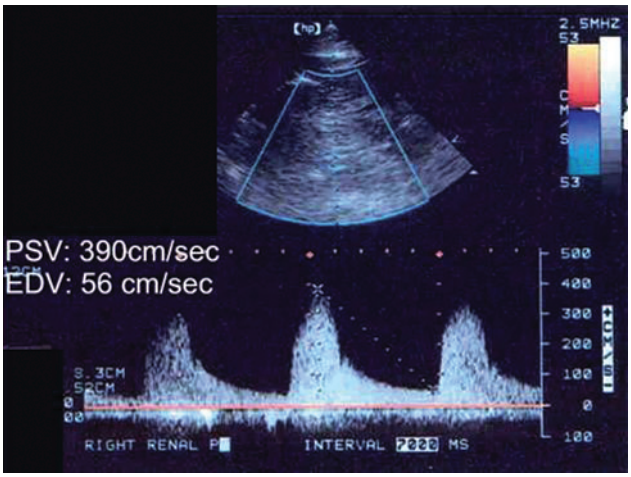

Figure 1.27 Renal-artery waveform in a patient with severe hypertension. The high PSV is compatible with a high-grade stenosis of the right renal artery.

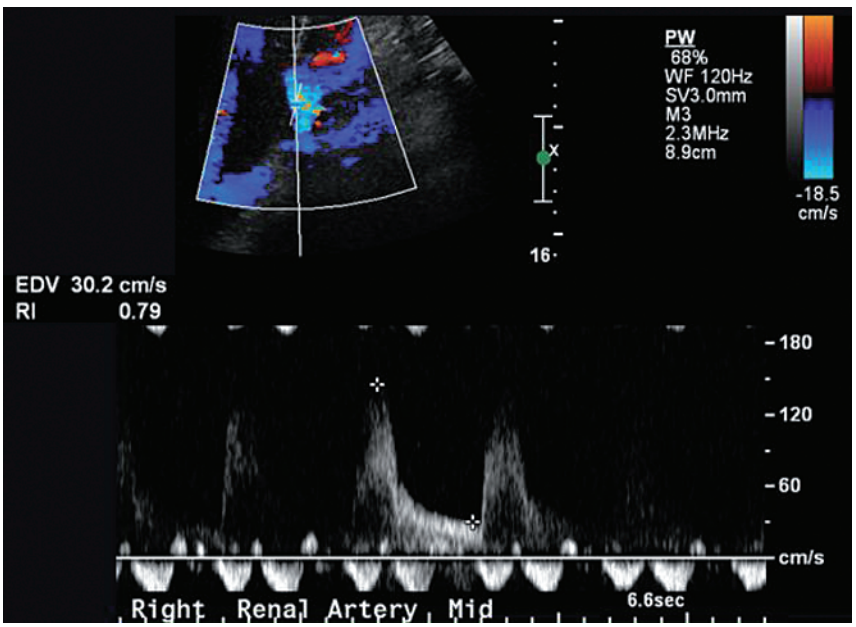

Figure 1.26 Normal renal-artery waveform. The PSV is under 185 cm/s and there is substantial forward flow at the end of diastole.

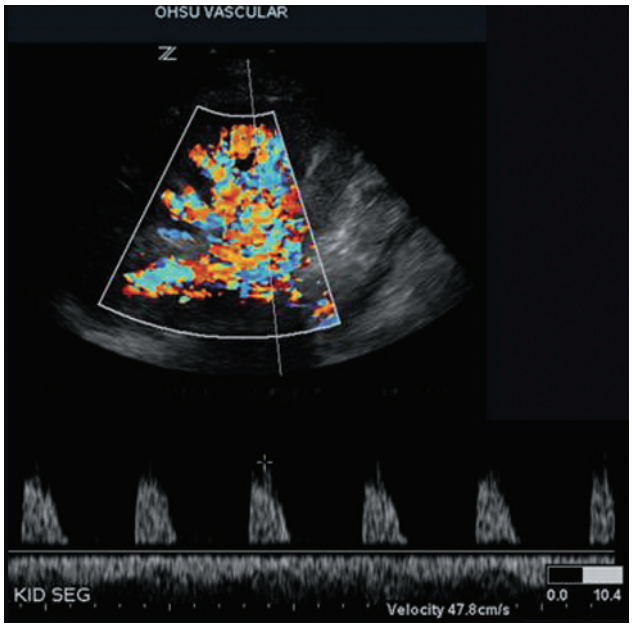

Figure 1.28 Absence of diastolic flow from the parenchyma of the kidney suggests parenchymal renal disease.

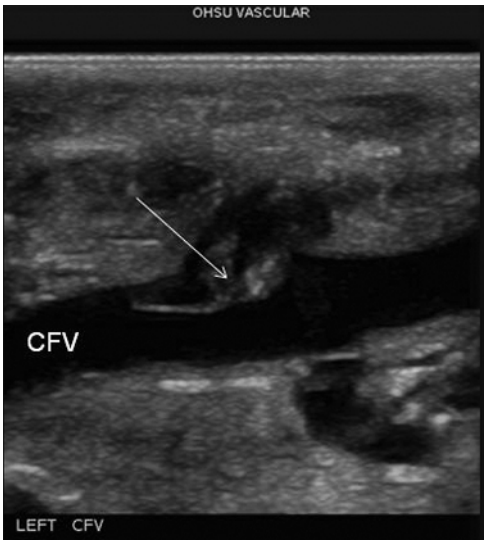

Figure 1.29 B-mode image of a saphenous vein thrombosis (arrow) extending into the common femoral vein (CFV).

blood flow. Decreased parenchymal diastolic flow may therefore suggest renal parenchymal disease (Fig. 1.28). Many patients with renal-artery stenosis treated with renal-artery revascularization do not have significant improvement in blood pressure or renal function. An estimate of resistance to flow within the renal parenchyma can be made using the EDV and PSV of renal-artery waveforms obtained from parenchymal arteries. The so-called resistive index (RI) is calculated as: $RI = [1–(EDV/PSV)] \times 100$. A high RI, >0.8, suggests renal parenchymal disease. A low RI indicates healthy renal parenchymal tissues. Evaluation of parenchymal resistance has been suggested as a possible pre-procedure predictor of clinical success of renal-artery interventions (59).

Venous disease

Acute deep venous thrombosis

Physical examination is not sensitive or specific for diagnosis of deep venous thrombosis (DVT) (60). Currently, color-flow duplex scanning performed by skilled operators provides the most practical and cost-effective method for assessment of DVT of the lower- and upper-extremity veins, as well as for superficial venous thrombosis.

A minimum duplex-ultrasound evaluation for lower-extremity DVT includes examination of the common femoral, profunda femoris, femoral, and popliteal veins (Fig. 1.29). Waveforms from the right and left common femoral veins should always be compared. A normal lower-extremity examination will show patency of the veins with color imaging, collapsing of the veins with application of pressure by the ultrasound probe, and flow patterns in the common femoral and femoral veins that decrease with inspiration and increase with expiration, and exhibit augmentation of flow with distal compression (Fig. 1.30). Flow within a patent vein should also increase with application of compression distal to the site of examination.

The primary ultrasound diagnostic criteria for acute venous thrombosis is failure of the vein to collapse with application of pressure with the ultrasound probe (Fig. 1.31). A continuous flow pattern in one common femoral vein and not the other suggests thrombosis or external compression of the ipsilateral iliac vein. Bilateral pulsatile common femoral-vein waveforms suggest volume overload, tricuspid regurgitation, or heart failure.

Not all venous ultrasound examinations for DVT are the same. Some vascular laboratories do not include evaluation of the calf veins even in symptomatic patients. This reflects outdated perceptions of inaccuracy of ultrasound evaluation for calf-vein DVT. If a complete initial examination including calf veins is not performed, serial ultrasound examinations or alternative strategies to detect possible extension of venous thrombi initially isolated to the calf veins must be employed. Such strategies, however, are inefficient, ineffective for non-compliant patients, and not cost effective compared with a single stand-alone color-flow duplex study of the proximal and calf veins.

Ultrasound studies for acute DVT may include compression ultrasound (B-mode imaging only), duplex ultrasound (B-mode imaging and Doppler waveform analysis), and color Doppler alone. The sensitivities and

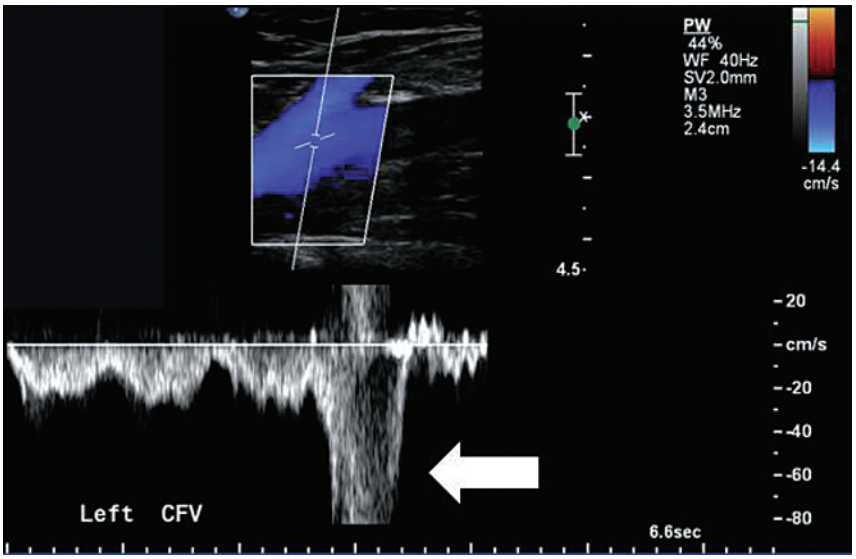

Figure 1.30 Proximal lower-extremity veins have flow that varies with respiration and augments with distal compression (arrow).

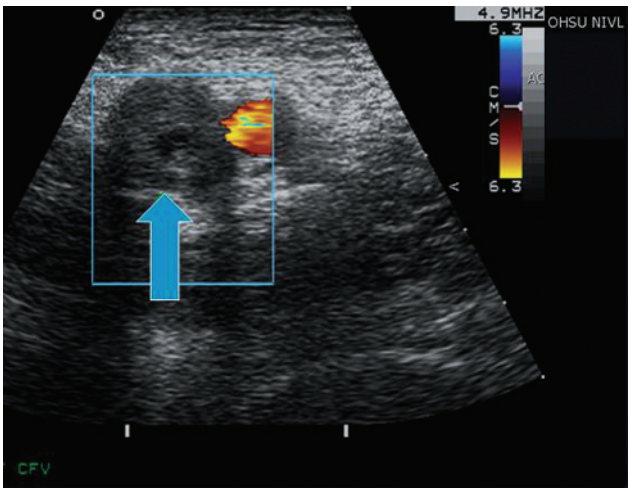

Figure 1.31 Failure of the common femoral vein to compress with pressure applied by the ultrasound scanhead indicates the presence of thrombus in the common femoral vein. As in this case, the acutely thrombosed vein is often enlarged and there is absence of collateral veins.

specificities for these examinations differ for detecting acute DVT. In the performance of a complete study different examinations are appropriate for different veins. Compression ultrasound is typically performed for evaluation of proximal deep veins, specifically the common femoral, femoral, and popliteal veins. A combination of duplex ultrasound and color Doppler is more often used for calf and iliac veins. Color flow alone may be used to assess patency of the calf veins as they are difficult to reliably compress, especially in subjects with large legs.

A complete color and Doppler examination has become the standard of care for assessment of lower-extremity DVT. It is recommended whenever possible, a venous duplex examination to exclude the presence of DVT consists of an evaluation of both the proximal and calf veins. However, many factors influence which venous segments can be evaluated in an individual examination. Morbid obesity, lower-extremity edema or tenderness, or the presence of immobilization devices and bandages may all limit a venous ultrasound examination for DVT. A well-trained technologist can interrogate calf veins in 80 to 98% of cases using a combination of B-mode, Doppler waveform analysis, and color Doppler (61, 62).

Overall accuracy of venous ultrasonography in comparison to venography is well established. The weighted mean sensitivity and specificity of venous ultrasonography (including all types) for the diagnosis of symptomatic proximal DVT are 97 and 94%, respectively (62). As suggested above, in technically adequate studies, the sensitivity and specificity of color Doppler to identify isolated calf-vein thrombosis exceeds 90% (62). The high specificity of venous ultrasonography allows treatment for DVT to be initiated without confirmatory tests, and the high sensitivity makes it possible to withhold treatment if the examination is negative.

When ultrasound examinations are limited by practical constraints an alternative procedure, such as catheter-based contrast venography, or MR or CT venography may be indicated. Repeat or serial venous ultrasound examinations are advisable for negative examinations in symptomatic patients highly suspicious for DVT, where an alternative form of imaging is unavailable or contraindicated.

A diagnosis of pulmonary embolism (PE), like that for DVT, also cannot be established without objective testing. Studies have evaluated the role of lower-extremity venous ultrasound examinations in patients suspected of PE. The rationale for venous ultrasonography in patients who present with symptoms of PE is that a diagnosis of DVT may indirectly suggest a diagnosis of PE, making additional investigation to exclude PE unnecessary in some clinical settings. However, ultrasound cannot make a definitive diagnosis of PE. Patients can have DVT and pulmonary symptoms, or hemodynamic instability from causes other than PE. In addition, normal bilateral proximal venous ultrasound scans do not rule out PE. When PE is definitively present, DVT of the proximal lower-extremity veins is detectable by compression ultrasound in only 50% of patients (63). When a PE is objectively diagnosed with no evidence of lower-extremity DVT, the PE may have originated from pelvic veins, arm veins, or possibly embolized completely from a lower-extremity vein. An objective diagnostic test for PE is therefore indicated in most cases. Currently, in most centers this would be a CT pulmonary angiogram.

Chronic venous insufficiency

Venous insufficiency can also be evaluated with duplex scanning and provides important physiologic and anatomic information in patients with possible chronic venous insufficiency (CVI) (64). Both sites of reflux and obstruction can be determined in deep, superficial, and perforating veins. In patients with valve incompetence, reflux can be stimulated and then detected with duplex scanning using a Valsalva maneuver, manual compression proximal to the transducer, or release of compression distal to the transducer. A standardized examination is performed with the patient upright and with the leg under examination non-weight bearing. The examination consists of insonation of the veins and assessment of reflux following deflation of a series of pneumatic cuffs at specific sites on the leg. Reflux stimulated by cuff deflation and lasting >0.5 s is indicative of pathologic reflux (65). The technique allows localization of reflux to specific venous segments and serves as a valuable preoperative planning tool to target specific venous segments for removal or reconstruction (Fig. 1.32). The cuff-deflation technique has a sensitivity of 82%, and specificity of 100% for the identification of incompetent perforating veins. Duplex determination of reflux sites and sites of venous occlusion as a means of assessing overall venous hemodynamics is not established. However, duplex assessment of venous reflux currently provides the basis of planning the large majority of venous procedures designed to treat manifestations of superficial venous reflux.

Selected miscellaneous examinations

Evaluation for abdominal aortic aneurysm

Vascular laboratory ultrasound screening of males >65 years with a history of cigarette smoking for abdominal aortic aneurysm (AAA) is effective in preventing aneurysm-related deaths in this cohort (66). Ultrasound is highly accurate and reproducible in measuring the diameter of infrarenal AAAs. Typically, patients with

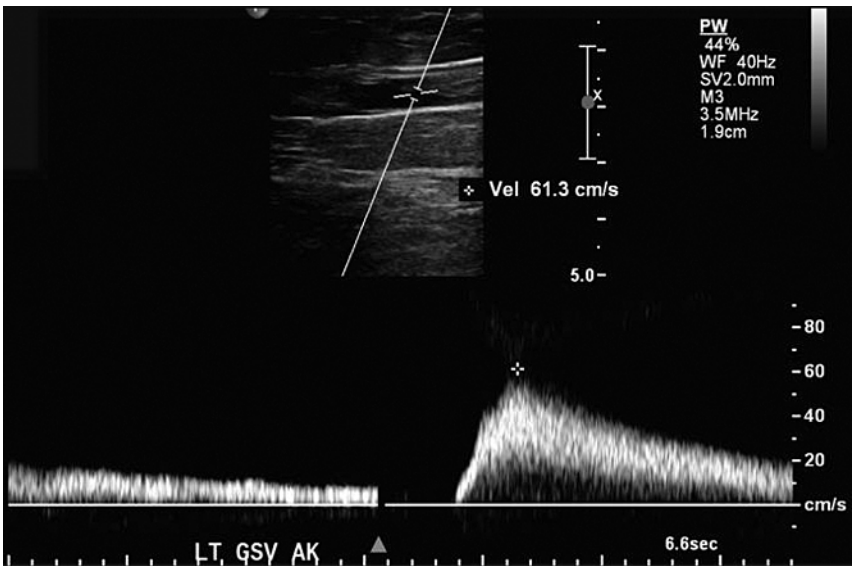

Figure 1.32 There is prolonged venous reflux (6.6 s) in this patient's greater saphenous vein following cuff deflation in the upright position. Venous reflux with this technique that extends >0.5 to 1 s is abnormal.

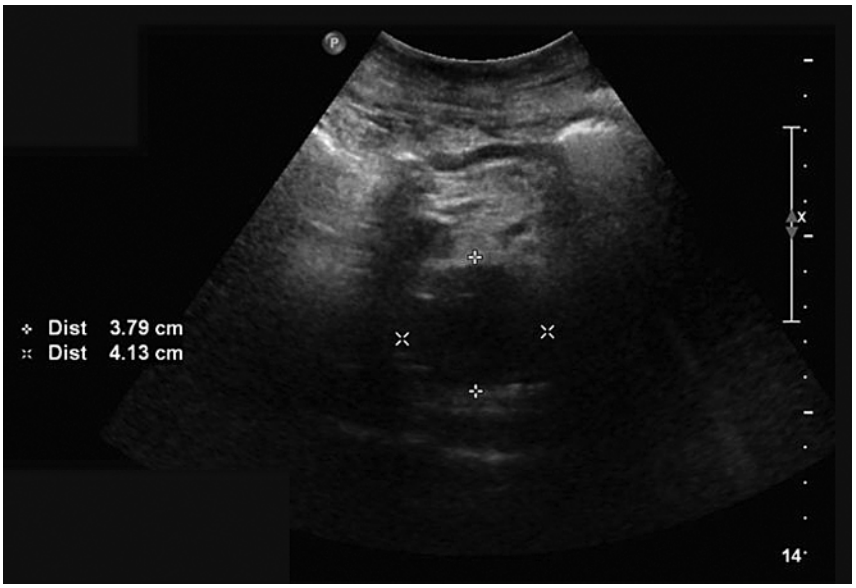

Figure 1.33 Surveillance ultrasound image of a small (4.13 cm diameter) infrarenal abdominal aortic aneurysm.

AAA diameters below accepted threshold levels for repair are followed with serial ultrasound examinations to monitor for enlargement of the aneurysm to a diameter where repair is indicated (Fig. 1.33).

Evaluation of aortic endografts

Placement of endoluminal stent grafts is standard therapy for most patients with AAA. The AAA is left in situ and blood flow diverted through the stent graft. Some stent grafts eventually leak at proximal or distal attachment sites. AAAs with these so-called type I endoleaks are at risk of rupture. In addition, AAAs treated with stent grafts may also occasionally enlarge because of back pressure in the aneurysm sac from patent lumbar vessels; type II endoleak. Patients whose AAAs enlarge in association with type II endoleaks after endografting are also considered at risk for aneurysm rupture.

Standard monitoring of endoluminal stent grafts consists of serial CT scans to detect endoleak and changing sac diameter. However, there are increasing concerns about repeated doses of contrast and radiation exposure associated with serial CT scans. It now appears many stent grafts can be followed with serial duplex-ultrasound examinations. In some centers duplex ultrasound has replaced CT scanning as the preferred method of follow-up of AAA stent grafts (67,68). Duplex ultrasound can measure sac diameter and detect type I and II endoleaks. An increase in sac diameter following stent grafting should prompt further investigation even if an endoleak itself is not detected.

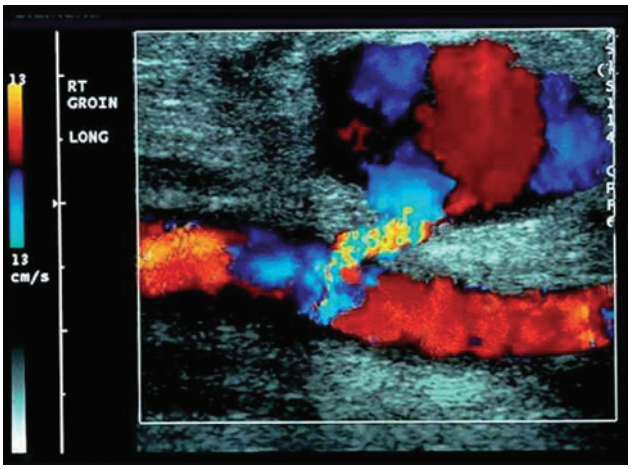

Figure 1.34 Color-flow image of a groin pseudoaneurysm. See text.

Evaluation and treatment of groin pseudoaneurysm

Groin pseudoaneurysms can occur as a complication of an arterial puncture in the groin. Groin pseudoaneurysms are readily detected with duplex ultrasound (Fig. 1.34). Color flow demonstrates flowing blood usually anterior to the artery from which the psuedoaneurysm originates. The native artery and psuedoaneurysm are connected by a "neck." To-and-fro flow within the neck of the pseudoaneurysm characterizes a one that is complicating an arterial puncture.

Treatment of pseudoaneurysms may be with direct surgical repair or, utilizing the vascular laboratory,

direct compression of the psuedoaneurysm with the ultrasound scanhead until it thromboses. Alternatively, the pseudoaneurysm is visualized with the ultrasound scanhead, a needle introduced into the body of the pseudoaneurysm, and small amounts of thrombin injected to induce thrombosis of the pseudoaneurysm (69,70). Currently, direct thrombin injection is favored as it is relatively noninvasive, less painful, and more effective than prolonged compression alone.

References

1. Roederer GO, Langlois YE, *et al*. Ultrasonic duplex scanning of the extracranial carotid arteries: Improved accuracy using new features from the carotid artery. *J Cardiovasc Ultrasonography* 1982;1:373.
2. Abou-ZamZam AM Jr, Moneta GL, *et al*. Is a single preoperative duplex scan sufficient for planning bilateral carotid endarterectomy? *J Vasc Surg* 2000;31:282.
3. Strandness DE Jr. Duplex scanning in vascular disorders. New York: Raven Press, 1990;92.
4. Roederer GO, Langlois YE, *et al*. A simple spectral parameter for accurate classification of severe carotid artery disease. *Bruit* 1989;3:174.
5. Moneta GL, Edwards JM, *et al*. Correlation of North American Symptomatic Carotid Endarterectomy Trial (NASCET): Angiographic definition of 70% to 90% internal carotid artery stenosis with duplex scanning. *J Vasc Surg* 1993;17:152.
6. Bendick PJ, Glover JL. Hemodynamic evaluation of the vertebral arteries by duplex ultrasouind. *Surg Clin North Am* 1990;70:235.
7. Kumar SM, Wang JC, *et al*. Carotid stump syndrome: outcome from surgical management. *Eur J Vasc Endovasc Surg* 2001;21:214.
8. North American Symptomatic Carotid Endarterectomy Trial Collaborators: NASCET: Beneficial effect of carotid endarterectomy in patients with high-grade carotid stenosis. *N Engl J Med* 1991;325:445.
9. European Carotid Surgery Trialists' Collaborative Group (ECST). MRC European Carotid surgery Trial: interim results for symptomatic patients with severe (70–99%) or with mild (0–29%) carotid stenosis. *Lancet* 1996;347:1591.
10. Mayberg MR, Wilson SE, *et al*. Carotid endarterectomy and prevention of cerebral ischemia in symptomatic carotid stenosis: Veterans Affairs Cooperative Studies Program 309 Trialist Group. *JAMA* 1991;266:3289.
11. Executive Committee for Asymptomatic Carotid Atherosclerosis Study: Endarterectomy for asymptomatic carotid artery stenosis. *JAMA* 1995;273:1421.
12. MRC Asymptomatic Carotid Surgery Trial (ACST) Collaborative Group. Prevention of disabling and fatal strokes by successful carotid endarterectomy in patients without recent neurological symptoms: randomized controlled trial. *Lancet* 2004;363:1491.
13. North American Symptomatic Carotid Endarterectomy (NASCET) Steering Committee: North American symptomatic carotid endarterectomy trial: Methods, patient characteristics, and progress. *Stroke* 1991;22:711.
14. Rothwell PM, Gibson RJ, *et al*. Equivalence of measurements of carotid stenosis: A comparison of three methods on 1001 angiograms. *Stroke* 1994;25:2435.
15. Moneta GL, Edwards JM, *et al*. Screening for asymptomatic internal carotid artery stenosis: Duplex criteria for discriminating 60% to 99% stenosis. *J Vasc Surg* 1995;21:989.
16. AbuRahma AF, Robinson PA, *et al*. Proposed new duplex classification for threshold stenoses used in various symptomatic and asymptomatic carotid endarterectomy trials. *Ann Vasc Surg* 1998;12:349.
17. Carpenter JP, Lexa FJ, Davis JT. Determination of duplex Doppler ultrasound criteria appropriate to the North American symptomatic carotid endarterectomy trial. *Stroke* 1996;27:695.
18. Hood DB, Mattos MA, *et al*. Prospective evaluation of new duplex criteria to identify 70% internal carotid artery stenosis. *J Vasc Surg* 1996;23:254.
19. Carpenter JP, Lexa FJ, Davis JT. Determination of 60% or greater carotid artery stenosis by duplex Doppler ultrasonography. *J Vasc Surg* 1995;22:697.
20. Browman MW, Cooperberg PL, *et al*. Duplex ultrasonography criteria for internal carotid stenosis of more than 70% diameter: Angiographic correlation and receiver operating characteristic curve analysis. *Can Assoc Radiol J* 1995;46:291.
21. Neale ML, Chambers JL, *et al*. Reappraisal of duplex criteria to assess significant carotid stenosis with special reference to reports from the North American symptomatic carotid endarterectomy trial and the European trial and the European carotid surgery trial. *J Vasc Surg* 1994;20:642.
22. Grant EG, Benson CB, *et al*. Carotid artery stenosis: Gray-scale and Dopler US diagnosis—Society of Radiologists in Ultrasound Consensus Conference. *Radiology* 2003;229:340.
23. Fujitani RM, Mills JL, *et al*. The effect of unilateral internal carotid arterial occlusion upon contralateral duplex study: Criteria for accurate interpretation. *J Vasc Surg* 1992;16:459.
24. Setacci C, Chisci E, *et al*. Grading Carotid Intra-Stent Re-Stenosis: A Six-Year Follow-Up Study. *Stroke* 2008;30:1189.
25. Slouvut DP, Romero JM, *et al*. Detection of common carotid stenosis using duplex ultrasonography: a validation study with computed tomographic angiography. *J Vasc Surg* 2010;51:65.
26. Moneta GL, Yeager RA, *et al*. Accuracy of lower-extremity arterial duplex mapping. *J Vasc Surg* 1992;15:275.
27. Jager KA, Ricketts HJ, Strandness DE. Duplex scanning for evaluation of lower-limb arterial disease. In Bernstein EF, ed. Noninvasive diagnostic techniques in vascular disease. St Louis: Mosby, 1985;619.
28. Whyman MR, Hoskins PR, *et al*. Accuracy and reproducibility of duplex ultrasound imaging in a phantom model of femoral artery stenosis. *J Vasc Surg* 1993;17:524.
29. Leng GC, Whyman MR, *et al*. Accuracy and reproducibility of duplex ultrasonography in grading femoropopliteal stenoses. *J Vasc Surg* 1993;17:510.
30. Sacks D, Robinson ML, *et al*. Peripheral arterial Doppler ultrasonography: diagnostic criteria. *J Ultrasound Med* 1992;11:95.
31. Jager KA, Phillips DJ, *et al*. Noninvasive mapping of lower-limb arterial lesions. *Ultrasound Med Biol* 1985;11:515.
32. Sensier Y, Hartshorne T, *et al*. A prospective comparison of lower-limb color-coded duplex scanning with arteriography. *Eur J Vasc Endovasc Surg* 1996;11:170.
33. de Smet AA, Ermers EJ, Kitslaar PJ. Duplex velocity characteristics of aortoiliac stenoses. *J Vasc Surg* 1996;23:628.
34. Elsman BH, Legemate DA, *et al*. Impact of ultrasonographic duplex scanning on therapeutic decision making in lower-limb arterial disease. *Br J Surg* 1995;82:630.

35. Ascher E, Mazzariol F, *et al*. The use of duplex ultrasound arterial mapping as an alternative to conventional arteriography for primary and secondary infrapopliteal bypasses. *Am J Surg* 1999;178:162.
36. Mazzariol F, Ascher E, *et al*. Values and limitations of duplex ultrasonography as the sole imaging method of preoperative evaluation for popliteal and infrapopliteal bypasses. *Ann Vasc Surg* 1999;13:1.
37. Larch E, Minar E, *et al*. Value of color duplex sonography for evaluation of tibioperoneal arteries in patients with femoropopliteal obstruction: a prospective comparison with anterograde intraarterial digital subtraction angiography. *J Vasc Surg* 1997;25:629.
38. Landry GJ, Moneta GL, *et al*. Patency and characteristics of lower-extremity vein grafts requiring multiple revisions. *J Vasc Surg* 2000; 32:23.
39. Johnson BL, Bandyk DF, *et al*. Intraoperative duplex monitoring of infrainguinal vein bypass procedures. *J Vasc Surg* 2000;31:678.
40. Idu MM, Blankenstein JD, *et al*. Impact of a color-flow duplex surveillance program on infrainguinal vein-graft patency: a five-year experience. *J Vasc Surg* 1993;17:42–52; discussion 52.
41. Lundell A, Lindblad B, *et al*. Femoropopliteal-crural graft patency is improved by an intensive surveillance program: a prospective randomized study. *J Vasc Surg* 1995;21:26–33; discussion 33.
42. Passman MA, Moneta GL, *et al*. Do normal early color-flow duplex surveillance examination results of infrainguinal vein grafts preclude the need for late graft revision? *J Vasc Surg* 1995;22:476–481; discussion 482.
43. Mills JL Sr, Wixon CL, *et al*. The natural history of intermediate and critical vein-graft stenosis: recommendations for continued surveillance or repair. *J Vasc Surg* 2001;33:273–278; discussion 278.
44. Yurdakul M, Tola M, Uslu OS. Color doppler ultrasonography in occlusive diseases of the brachiocephalic and proximal subclavian arteries. *J Ultrasound Med* 2008;27: 1065.
45. Strandness DE. Duplex scanning in vascular disorders. New York: Raven Press, 1993:159.
46. Grosveld WJ, Lawson JA, *et al*. Clinical and hemodynamic significance of innominate artery lesions evaluated by ultrasonography and digital angiography. *Stroke* 1988;19: 958.
47. Reed AJ, Fincher RME, Nichols FT. Case report: Takayasu's arteritis in a middle-aged Caucasian woman: clinical course correlated with duplex ultrasonography and angiography. *Am J Med Sci* 1989;298:324.
48. Jagar KA, Fortner GS, *et al*. Noninvasive diagnosis of intestinal angina. *J Clin Ultrasound* 1984;12:588.
49. Gentile AT, Moneta GL, *et al*. Fasting and postprandial superior mesenteric artery duplex scanning in the diagnosis of high-grade superior mesenteric artery stenosis. *Am J Surg* 1995;169:476.
50. Moneta GL, Taylor DC, *et al*. Duplex ultrasound measurement of postprandial intestinal blood flow: Effect of meal composition. *Gastroenterology* 1998;95:1294.
51. Moneta GL, Lee RW, *et al*. Mesenteric artery duplex scanning: a blinded prospective study. *J Vasc Surg* 1993;17: 79.
52. Zwolak, RM, Fillinger MF, *et al*. Mesenteric and celiac duplex scanning: a validation study. *J Vasc Surg* 1998;27: 1078.
53. Liem TK, Segall JA, *et al*. Duplex scan characteristics of bypass grafts to mesenteric arteries. *J Vasc Surg* 2007;45:922.
54. Mitchell EL, Chang EY, *et al*. Duplex criteria for native superior mesenteric arteries stenosis overestimates stenosis in stented superior mesenteric arteries. *J Vasc Surg* 2009;50:335.
55. Taylor DC, Kettler MD, *et al*. Duplex ultrasound in the diagnosis of renal artery stenosis: a prospective evaluation. *J Vasc Surg* 1998;7:363.
56. Hoffman U, Edwards JM, *et al*. Role of duplex scanning for detection of atherosclerotic renal artery disease. *Kidney Int* 1991;39:1232.
57. Olin JW, Piedmonte MR, *et al*. The utility of duplex ultrasound scanning of the renal arteries for diagnosing significant renal artery stenosis. *Ann Intern Med* 1995;122:833.
58. Mohabbat W, Greenerg RK, *et al*. Revised duplex criteria and outcomes for renal stents and stent grafts following endovascular repair of juxtrarenal and thoracoabdominal aneurysms. *J Vasc Surg* 2009;49:827.
59. Radermacher J, Chavan A, *et al*. Use of Doppler ultrasonography to predict the outcome of therapy for renal-artery stenosis. *New Engl J Med* 2001;344:410.
60. Wells PS, Hirsh J, Anderson DR. Accuracy of clinical assessment of deep-vein thrombosis. *Lancet* 1995;345:1326.
61. Schindler JM, Kaiser M, *et al*. Color coded duplex sonography in suspected deep vein thrombosis. *Br J Surg* 1991;78:611.
62. Rose SC, Zwiebel WJ, *et al*. Symptomatic lower-extremity deep venous thrombosis: accuracy, limitations, and role of color duplex flow imaging in diagnosis. *Radiology* 1990; 175:639.
63. Kearon C. Diagnosis of pulmonary embolism. *CMAJ* 2003;168:183.
64. Welch Hg, Faliakou EC, *et al*. Comparison of descending phlebography with quantitative photoplethysmography, air plethysmography and duplex quantitative valve closure time in assessing deep venous reflux. *J Vasc Surg* 1989;10:425.
65. van Bemmelen PS, Bedford G, *et al*. Quantitative segmental evaluation of venous valvular reflux with duplex ultrasound scanning. *J Vasc Surg* 1989;10:425.
66. Fleming C,Whitlock EP, *et al*. Screening for abdominal aortic aneurysm: a best evidence systematic review for the U.S. preventive services task force. *Ann Intern Med* 2005; 142:203.
67. Sanford RM, Brown MJ, *et al*. Duplex ultrasound scanning is reliable in the detection of endoleak following endovascular aneurysm repair. *Eur J Vasc Endovasc Surg* 2006;32:537.
68. Chaer RA, Gushchin A, *et al*. Duplex ultrasound as the sole long-term surveillance method post endovascular aneurysm repair: a safe alternative for stable aneurysms. *J Vasc Surg* 2009;49:845.
69. Cox GS, Young JR, *et al*. Ultrasound guided compression repair of postcatheterzation pseudoaneurysms: results of treatment in 100 cases. *J Vasc Surg* 1994;19:683.
70. Kang SS, Labropoulos N, *et al*. Expanded indications for ultrasound guided thrombin injection of pseudoaneurysms. *J Vasc Surg* 2000;31:289.